J. Micropalaeontology, 42, 95–115, 2023
https://doi.org/10.5194/jm-42-95-2023

Journal of Micropalaeontology
Open Access

Paleoenvironmental changes related to the variations of the sea-ice cover during the Late Holocene in an Antarctic fjord (Edisto Inlet, Ross Sea) inferred by foraminiferal association

Giacomo Galli[1,2], Caterina Morigi[2], Romana Melis[3], Alessio Di Roberto[4], Tommaso Tesi[5], Fiorenza Torricella[6], Leonardo Langone[5], Patrizia Giordano[5], Ester Colizza[3], Lucilla Capotondi[7], Andrea Gallerani[7], and Karen Gariboldi[1]

[1]Dipartimento di Scienze Ambientali, Informatica e statistica, Università Ca' Foscari Venezia, Via Torino 155, 30172, Venice, Italy
[2]Dipartimento di Scienze della Terra, Università di Pisa, Via Santa Maria, 53, 56126, Pisa, Italy
[3]Dipartimento di Matematica e Geoscienze, Università di Trieste, Via E. Weiss 2, 34127, Trieste, Italy
[4]Istituto Nazionale di Geofisica e Vulcanologia (INGV), Sezione di Pisa, Via della C, Battisti 53, 56125, Pisa, Italy
[5]Istituto di Scienze Polari – Consiglio Nazionale delle Ricerche ISP-CNR, Via P. Gobetti 101, 40129, Bologna, Italy
[6]Istituto Nazionale di Oceanografia e di Geofisica Sperimentale (OGS), Borgo Grotta Gigante 42/c, 34010, Sgonico, Trieste, Italy
[7]Istituto di Scienze Marine – Consiglio Nazionale delle Ricerche ISMAR-CNR, Via P. Gobetti 101, 40129, Bologna, Italy

Correspondence: Giacomo Galli (giacomo.galli@unive.it)

Received: 5 May 2023 – Revised: 11 August 2023 – Accepted: 20 August 2023 – Published: 13 September 2023

Abstract. TR17-08, a marine sedimentary core (14.6 m), was collected during 2017 from the Edisto Inlet (Ross Sea, Antarctica), a small fjord near Cape Hallett. The core is characterized by expanded laminated sedimentary sequences making it suitable for studying submillennial processes during the Early Holocene. By studying different well-known foraminifera species (*Globocassidulina biora, G. subglobosa, Trifarina angulosa, Nonionella iridea, Epistominella exigua, Stainforthia feylingi, Miliammina arenacea, Paratrochammina bartrami* and *Portatrochammina antarctica*), we were able to identify five different foraminiferal assemblages over the last ∼2000 years BP. Comparison with diatom assemblages and other geochemical proxies retrieved from nearby sediment cores in the Edisto Inlet (BAY05-20 and HLF17-1) made it possible to distinguish three different phases characterized by different environmental settings: (1) a *seasonal phase* (from 2012 to 1486 years BP) characterized by the dominance of calcareous species, indicating a seasonal opening of the inlet by more frequent events of melting of the sea-ice cover during the austral summer and, in general, a higher-productivity, more open and energetic environment; (2) a *transitional phase* (from 1486 to 696 years BP) during which the fjord experienced less extensive sea-ice melting, enhanced oxygen-poor conditions and carbonate dissolution conditions, indicated by the shifts from calcareous-dominated association to agglutinated-dominated association probably due to a freshwater input from the retreat of three local glaciers at the start of this period; and (3) a *cooler phase* (from 696 years BP to present) during which the sedimentation rate decreased and few to no foraminiferal specimens were present, indicating ephemeral openings or a more prolonged cover of the sea ice during the austral summer, affecting the nutrient supply and the sedimentation regime.

Published by Copernicus Publications on behalf of The Micropalaeontological Society.

1 Introduction

The Antarctic region is currently characterized by a sea-ice cover with a high degree of variability, both temporally and spatially (Eayrs et al., 2019). Over the last 4 decades, various trends have been observed throughout different Antarctic regions: the Ross Sea region has experienced an increase in the sea-ice cover of 2.4 %, in contrast to the Bellingshausen–Amundsen Sea region, where the cover experienced a decrease of about 3.1 % (Maksym, 2019). Overall, the Antarctic sea ice is experiencing a positive trend, which is not reproduced by climate models (Turner et al., 2013, 2015). In addition to this, the observed trend might not be linear. In 2016, the interplay between El Niño and the Southern Annular Mode produced a decrease of the sea-ice coverage of ∼ 28 %, leading to the recorded year with the lowest sea-ice extent and the earliest onset of the melting (August) (Turner et al., 2017; Schlosser et al., 2018) . This type of variability leads to difficulties in modelling and interpretation of the climatic oscillations that this region experienced, especially in regional climate models, where the sea-ice cover is a parameter that yields the highest uncertainties (Meehl et al., 2014; Rosenblum and Eisenman, 2017). In addition, sea-ice variability affects marine communities, being the main factor that controls primary producer associations (van Leeuwe et al., 2018). Therefore, studying how the sea-ice cover has evolved could shed light on the process that governs this variability, in addition to offering a more comprehensive and detailed view of the Antarctica climate evolution. To fill this gap on climate sea-ice interactions, several projects focused on the last 2000 years (i.e. Past Global Changes-PAGE 2K), trying to connect field observations with climate models to obtain a more precise view of the process that regulates the Antarctic climate system. Within this framework, in this study, we focus on the environmental changes over the last 2000 years in Edisto Inlet (Ross Sea, Antarctica), a little fjord situated along Victoria Land, in the western Ross Sea. We decided to focus mainly on the transition between two highly studied climatic periods: the Medieval Climate Anomaly and the Little Ice Age (Stenni et al., 2017; Lüning et al., 2019). This fjord was previously investigated by Finocchiaro et al. (2005), Mezgec et al. (2017) and Tesi et al. (2020), focusing on the difference in laminae composition of cores collected in the bay, showing the potential for high-resolution studies. Specifically, Tesi et al. (2020) suggested that the lamination along the cores reflects different sea-ice cover scenarios, where a dark lamina indicates a first break-up of the sea ice during the early summer, followed by a light lamina indicating a protracted ice-free condition. From a paleoclimatic point of view, Tesi et al. (2020) were able to identify a period of marked seasonality of the sea-ice cover (from ∼ 2100 to ∼ 700 years BP), followed by a period with a multi-year sea-ice cover (∼ 700 years BP to recent), possibly linked to atmospheric cooling (Stenni et al., 2017). Di Roberto et al. (2019) and Di Roberto et al. (2023) focused on cryptotephra layers in the sediment cores, used to build more robust age–depth models. In this work, we analyse the shifts in composition of the foraminifera assemblages along core TR17-08 to reconstruct the past environmental, climatic and oceanographic conditions that affected the Edisto Inlet during the last 2000 years. The overreaching goal was to show the potential of foraminiferal studies in high-resolution settings in Antarctica.

2 Regional setting

2.1 Ross Sea oceanographic setting

The Ross Sea is an Antarctic marine region defined by the Ross Ice Shelf to the south and by the 700 m isobath to the north, with an average depth of ca. 530 m and a maximum depth of about 1000 m, located in the Drygalski Trough region (Orsi and Wiederwohl, 2009; W. Smith et al., 2012). The Ross Sea is currently characterized by the presence of a sea-ice cover, which is related to the behaviour of the two main polynyas: the Terra Nova Bay polynya and the Ross Sea polynya. The sea-ice grows, in both concentration and thickness, during austral winter and melts during austral summer (Fraser et al., 2012; Parkinson and Cavalieri, 2012; W. O. Smith et al., 2012; R. W. Smith et al., 2015). The input of water masses in this region is dominated by the Ross Gyre activity, a cyclonic current system located north of the Ross Sea, and by the Antarctic Slope Current, which flows westward along the 700 m steep slope. The input of the Antarctic Surface Water (AASW), a cold and rather fresh water mass, is found near Cape Colbeck, where it flows westward along the Ross Ice Shelf (Orsi and Wiederwohl, 2009; W. Smith et al., 2012; W. O. Smith et al., 2014; Dotto et al., 2018). A layer of a warm water mass, named Circumpolar Deep Water (CDW), flows westward along the slope and cannot easily enter the Ross Sea due to poleward-diving isopycnals located at the 700 m slope (Ainley and Jacobs, 1981). The mixing of Circumpolar Deep Water with the Antarctic Circumpolar Current and the shelf water masses forms the Modified Circumpolar Deep Water (mCDW), which flows from the shelf break to the coastline (Castagno et al., 2017; Gales et al., 2023). Atmospheric cooling promotes sea-ice formation, which increases surface salinity and enhances the production of sinking high-salinity shelf water (HSSW), which covers most of the Ross Sea and Ross Ice Shelf bottom layers (W. Smith et al., 2012). This water mass flows northward, facilitating the entrance of the mCDW, especially in the western and central part of the Ross Sea (Ainley and Jacobs, 1981; Orsi and Wiederwohl, 2009; W. Smith et al., 2012). In the Drygalski, JOIDES and Glomar Challenger basins, the formation and outflow of the HSSW, and the subsequential mixing with the layer of mCDW at the shelf break, form the

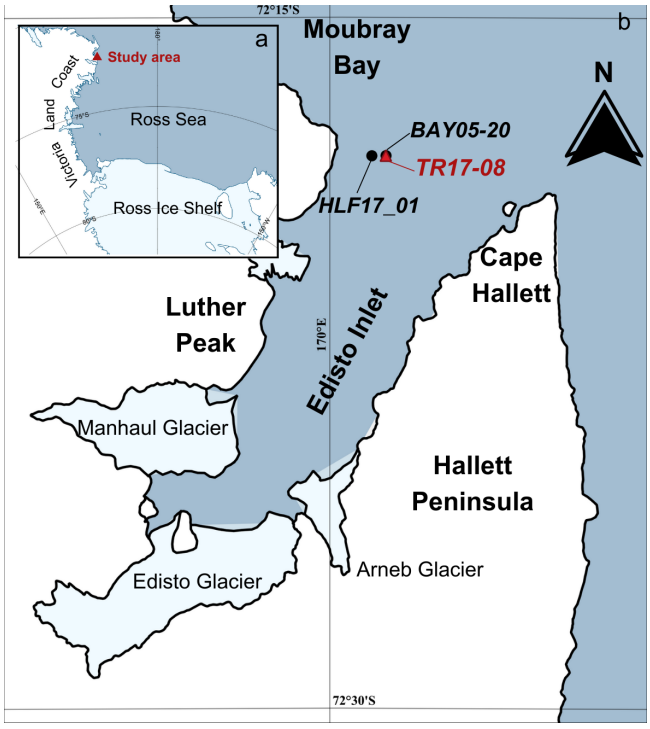

Figure 1. Study area. **(a)** Ross Sea and study area (red triangle) and **(b)** location of the marine cores from this study, TR17-08 (red triangle) and the two other marine cores collected in this area: HLF17-1 (Tesi et al., 2020) and BAY05-20 (Mezgec et al., 2017) (black dots). Map compiled with Quantarctica (Matsuoka et al., 2021).

modified shelf water (a warmer, more salty water mass than HSSW), which continues to sink once passed the slope break, forming the Antarctic Bottom Water (AABW), which is one of the most important water masses exported by the Ross Sea, providing nutrients at lowers latitudes (Whitworth and Orsi, 2006; W. Smith et al., 2012; W. O. Smith et al., 2014).

2.2 Edisto inlet setting

The Edisto Inlet is a fjord situated near Cape Hallett, in the north-western part of the Ross Sea, characterized by the presence of a seasonal sea-ice cover and expanded Holocene sedimentary sequence mainly composed of soft biogenic lamination (Finocchiaro et al., 2005; Mezgec et al., 2017; Di Roberto et al., 2019; Tesi et al., 2020). The fjord is 4 km wide and 15 km long, elongated in the NNE–SSW direction, with a maximum depth of about 500 m, where three main glaciers converge (Manhaul Glacier, Arneb Glacier and Edisto Glacier; Fig. 1).

2.3 Foraminifera from the western Ross Sea

The Antarctic foraminiferal assemblages are mainly dependent on sea-ice cover, type of substrate, bottom currents, primary productivity, and physical and chemical properties of the water column and the carbonate compensation depth (CCD) (Anderson, 1975; Ward et al., 1987; Mackensen et al., 1990; Ishman and Sperling, 2002; Majewski, 2010; Capotondi et al., 2020). In modern Antarctica marginal settings, the average depth of the CCD is ∼ 550 m, although this varies depending on the physio-chemical characteristics of the area. A modification of the environmental parameters could lead to a change in the composition of the benthic foraminifera assemblage, highlighting the key role that this group has in paleoceanographic and paleoclimatic reconstruction. The western Ross Sea benthic assemblages are composed of agglutinated and calcareous forms (Ward et al., 1987; Violanti, 2000; Melis and Salvi, 2009; Capotondi et al., 2020; Melis and Salvi, 2020). Studies on living and dead benthic assemblages along the coast of the western Ross Sea show the presence of two main associations: one dominated by the genus *Globocassidulina*, a calcareous taxon found in high-energy environment above the CCD often found in settings with coarser substrate (Li et al., 2000; Majewski et al., 2018), and the other dominated by agglutinated forms, mainly by the *Trochammina* group and *Miliammina arenacea*, associated with mud-type substrate. This latter assemblage is found below the CCD, and it is indicative of a low-energy, high-productivity environment (Ward et al., 1987; Brambati et al., 2000; Violanti, 2000; Majewski and Anderson, 2009; Capotondi et al., 2020). Regarding the planktic foraminifera assemblages, one species dominates the western part of the Ross Sea: *Neogloboquadrina pachyderma* (Bergami et al., 2009), which is able to thrive into the sea ice, in the ice–water boundary and in the granular ice of the brine (Hilbrecht, 1997). Mostly feeding on diatoms, this species thrives in high-productivity settings, especially below the deep chlorophyll maximum, between 50 and 100 m (Asioli and Langone, 1997; Bergami et al., 2009; Schiebel and Hemleben, 2017).

3 Methods

3.1 Core description

The piston core (TR17-08) was retrieved in January 2017, in the frame of the TRACERS project funded by the Italian National Programme for Antarctic Research (PNRA), at a depth of 462 m, with a length of 14.5 m, in the proximity of the entrance of the fjord (−72°18.2778 N, 170°04.1784 E; Fig. 1). The core is mainly composed of diatomaceous ooze with the presence of light and dark laminae from the bottom to the top. In Edisto, the colour of the lamina represents different diatom assemblages: light laminae are dominated by *Corethron pennatum*, whereas dark laminae are constituted by *C. pennatum*, *Fragilariopsis curta* and *F. obliquecostata*

(Tesi et al., 2020; Di Roberto et al., 2023). The lamination is not homogeneous in both the colour and thickness of the laminae, with the light-colour laminae becoming less evident in the upper portion (Fig. 2). The core was divided on board into 15 main sections: 14 sections with a length of 1 m and 1 shorter section with a length of 63 cm (Fig. 2). Every section was stored on the vessel at 4 °C after its collection. For the present study, we performed micropaleontological analyses on sections XV–IX (0–650.5 cm) corresponding to the last ∼ 2000 years (Di Roberto et al., 2023).

3.2 Radiocarbon chronology

Within core TR17-08, 10 intervals of high-concentration carbonate material (i.e. echinoids, ophiuroid ossicles and foraminifera tests) were chosen for radiocarbon dating (Table 1). The selected carbonate material (> 1 mg) came from samples 1 cm thick (except for the 61–63 cm interval), washed with distilled water using a sieve mesh of 63 µm and then stored at 40 °C for 12 h to dry. The radiocarbon analyses were performed at the MICADAS laboratory (Alfred Wagner Institute, Germany). In this study we use the age–depth model developed by Di Roberto et al. (2023) (Fig. 3).

3.3 Sample processing

A total of 71 samples (1 cm thickness) were retrieved from TR17-08 every 5 cm in the interval between 0–40 cm and every 10 cm in the 40–650 cm interval. Samples were weighed with a precision scale (0.001 g), washed with a 63 µm mesh, and the upper fraction was collected in filter paper. The samples were stored in a oven at 40 °C overnight to dry. We weighed the fraction greater than 63 µm. A column of sieves (with a mesh size of 1 mm and 150 µm) was used to separate the dry fraction > 150 µm from the finer fraction (63–150 µm). The fraction 63 µm was collected and will be investigated in future studies. The foraminifera study was performed using a stereomicroscope (Leica MZ 12.5) on the fraction > 150 µm. The samples were stored in foraminiferal microslides, identified and counted following the taxonomy of Anderson (1975), Mackensen et al. (1990), Violanti (2000), Igarashi et al. (2001) and Majewski et al. (2018). Some foraminifera were analysed at the scanning electron microscope (Hitachi TM3030plus Scanning Electronic Microscope) to evidence details of superficial microtexture and structure. Abundances of benthic foraminifera are relative to the total of the benthic specimens; planktic abundances were calculated relative to the total of the foraminifera specimens. The benthic foraminifera accumulation rate (BFAR) was calculated for benthic species using the equation from Herguera and Berger (1991). We conducted a principal component analysis (PCA). PCA is a frequently used technique in micropaleontology, being able to transform a large set of ecological variables into a smaller set of orthogonal components (Abdi and Williams, 2010). PCA scores represent how a variable contributes to a particular component and can be useful to define significant species, assuming the relationship between high score and ecological characteristics of the species (Kyrmanidou et al., 2018; Majewski et al., 2018). Loading coefficients represent the correlation between the sample and the component. Following Malmgren and Haq (1982) loading values above 0.4 were considered significant. The PCA in this study was performed using the benthic species that appears more than once and has an abundance above or equal to 2 % of the total assemblages. We use Past 4.11 to perform the analysis (Hammer et al., 2001).

4 Results

4.1 Foraminiferal content

Along the studied section, 45 species were identified, divided into 25 genera, among which only 1 species (*Neogloboquadrina pachyderma*) is planktic (Table 2). The number of benthic and planktic foraminifera specimens decreases from the bottom to the top, with the highest values (∼ 553 specimens g^{-1}) reached at 1960 ± 297 years BP, and the lowest value (0 specimens) is reached at 861 ± 191 years BP and at the top of the core (Fig. 4). Perforate calcareous species continuously dominate the assemblages, from the bottom of the studied sections (2012 ± 298 years BP) to 1394 ± 237 years BP (Fig. 4). Agglutinated benthic species, such as *Labrospira jeffreysii*, *Portatrochammina bartrami*, *Paratrochammina antarctica* and *Miliammina arenacea*, are present throughout the core, from 1394 ± 237 years BP to the top of the core (Fig. 4).

4.2 Principal component analysis (PCA)

Results of PCA show that the first two principal components (PCs) account for 86.2 % of the total variance, with the first one explaining 63.4 % and the second one explaining 22.8 % of the total variance (Table 3). The name of the PC was given by the species with the highest scores and described as foraminiferal assemblages (FAs). The first PC (*G. biora*, FA) shows a high score with *Globocassidulina biora* (4.48); the second PC (*P. antarctica* and *P. bartrami* FA) shows a high score for both *Paratrochammina bartrami* (3.67) and *Portatrochammina antarctica* (2.41) (Table 4). The loading distribution of these two FAs throughout the studied section permitted us to identify a period with the *G. biora* FA well above the significance threshold (2012 ± 298–1186 ± 243 years BP; Fig. 5a) and a period where the *P. antarctica*/*P. bartrami* FA was well above the threshold (953 ± 214.5–696 ± 23.5 years BP; Fig. 5b). The interval between these two periods (1186 ± 243–956 ± 214.5 years BP) shows a complicated relationship between the *G. biora* FA and *P. antarctica*/*P. bartrami* FA, with isolated peaks of both FA above the significance threshold. In addition, the period that goes from 687 ± 16 years BP to the present is difficult to

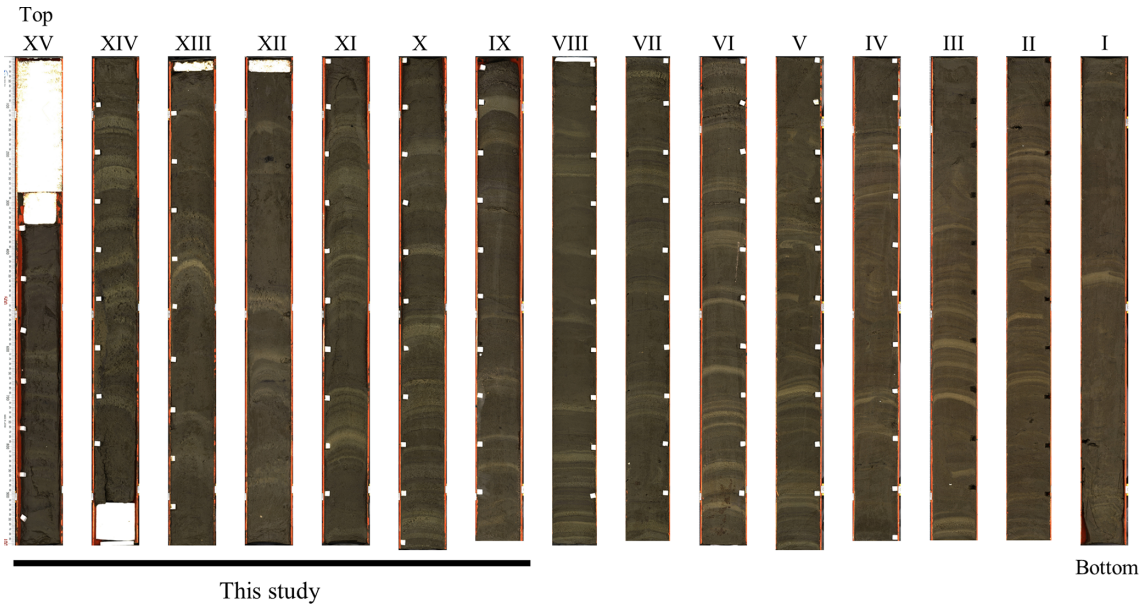

Figure 2. TR17-08 core, with enumerated sections, from top (XV) to bottom (I). The sections used in this study are highlighted by the horizontal black line.

Table 1. Dates used to build the age–depth model (Di Roberto et al., 2023). Data include both radiocarbon dates and tephra (*). Along with the age, the sample name, the absolute depth, the source, the relative error and the offset (ΔR) are displayed. The ages are reported with the application of the ΔR in the investigated area (Di Roberto et al., 2023).

Sample	Depth (cm)	Material	Age (years BP)	Error (± years)
XV 55–56*	55.5	tephra	687	14
XV 61–63	62	echinoid	801	247.5
XIII 78–79	234.5	echinoid	1075	260
X 13–14	463.5	ophiuroid	1416	256.5
X 61–63	512	foraminifera	1374	342.5
X 66–69	517.5	foraminifera	1743	350
X 74–75	524.5	foraminifera	1770	351
X 75–76	525.5	foraminifera	1782	354,5
VIII 77–78	729.5	ophiuroid	2242	359
VI 12–13	863.5	echinoid	2621	304
I 17–18	1369.5	scaphopod	3376	328

interpret due to the low number of foraminiferal specimens found. To disentangle the relationship between these two FAs, in addition to the PCA results, we selected other well-studied foraminifera species to describe a more detailed and comprehensive view of the environmental evolution of this site (Table 4, Appendix A). These species were selected due to their ecological characteristics and relative abundances.

4.3 Foraminiferal association

To distinguish between the FA derived from the results of the PCA and the foraminiferal assemblages recognized using the species in Table 4, the latter are regarded as foraminiferal association (FoA). Over the last 2012 years BP we recognized the presence of five FAs (Figs. 6 and 7). Each of the five FoAs was constrained based on the accumulation fluxes (Fig. 6) and the relative abundances (Fig. 7) of planktic and benthic foraminifera species indicated in Table 4. The foraminiferal associations are described in stratigraphical order.

4.3.1 Foraminiferal association E: 2012 ± 298–1486 ± 200 years BP

This FoA is defined by the presence of *Epistominella exigua*, *Nonionella iridea*, *Trifarina angulosa* and *Neogloboquadrina pachyderma* and by the highest fluxes of *Globocassidulina biora* together with *G. subglobosa*, the latter increasing from the bottom to the upper limit of this interval (Fig. 6). In addition, the relative abundance of the *Globocassidulina* group (*G. biora* and *G. subglobosa*) is constantly

Table 2. Identified benthic foraminifera species from the core TR17-08. The species are divided by their test characteristics: agglutinated, calcareous imperforate and calcareous perforate.

Test	Species	
Agglutinated	*Labrospira jeffreysii*	*Paratrochammina bartrami*
	Miliammina arenacea	*P. bipolaris**
	M. oblunga	*Pseudotrochammina arenacea**
	Paratrochammina tricamerata	*Trochammina multiloculata**
	P. nana	*Rhumblerella* sp.
	Portatrochammina antarctica	
Calcareous imperforate	*Pyrgo depressa*	*Q. weaveri*
	*P. williamsoni**	*Quinqueloculina* spp.*
	*Quinqueloculina seminula**	
	*Q. venusta**	
Calcareous perforate	*Astrononion echolsi*	*Melonis barleeanum**
	Astrononion antarcticus	*Nonionella iridea*
	Cassidulinoides porrectus	*N. bradii*
	*Cibicides lobatulus**	*N. magnalingua*
	C. refulgens	*Nonionella* sp.*
	Epistominella exigua	*Oolina exagona**
	*Fissurina semimarginata**	*Procelarogena multilatera**
	Fissurina spp.*	*Pullenia quinqueloba**
	Globocassidulina biora	*Rosalina globularis*
	G. crassa	*R. villaderboana**
	G. subglobosa	*Stainforthia feylingi*
	Globocassidulina spp.	*Stainforthia* sp.*
	*Heronallenia kempii**	*Trifarina angulosa*
	*Hyalinonetrion sahulense**	*Neogloboquadrina pachyderma*

* Rare species that appear once and/or have a relative abundance < 2 %.

above 50 % of the benthonic association (Fig. 7). *E. exigua*, *N. iridea* and *N. pachyderma* abundances and fluxes reach their highest values during this interval (Figs. 6 and 7).

4.3.2 Foraminiferal association D: 1486 ± 200–1317 ± 248.5 years BP

This FoA is characterized by the sharp increase of the accumulation fluxes of both *Stainforthia feylingi* and the agglutinated species *Miliammina arenacea* (Fig. 7). The upper limit of this interval is defined by the almost complete disappearance of *G. subglobosa* and *T. angulosa*. With respect to the previous association, this FoA shows an abrupt decrease in fluxes and abundances of *G. subglobosa* and the disappearance of *E. exigua* (Fig. 6). During this interval, agglutinant species, such as *Portatrochammina antarctica* and *Paratrochammina bartrami*, show an increase in relative abundance and a higher accumulation flux (Figs. 6 and 7). Lastly, *N. pachyderma* accumulation fluxes and abundances are lower than the previous FoA.

4.3.3 Foraminiferal association C: 1317 ± 248.5–953 ± 214.5 years BP

This FoA is defined by the presence of *G. biora*, *P. bartrami*, *P. antarctica*, *S. feylingi*, *M. arenacea* and *N. pachyderma*. The upper limit is defined by the disappearance of *G. biora*, *S. feylingi* and of the only planktic species, *N. pachyderma* (Figs. 6 and 7). During this interval, *G. biora* fluxes show a different behaviour than in the previous ecozones, with a more variable presence, exacerbated by the presence of two isolated peaks. *P. antarctica* and *P. bartrami* show a gradual increase in relative abundances, and the accumulation flux values are comparable with the FoA D (Fig. 6). *T. angulosa*, *E. exigua* and *N. iridea* appear once during this interval. *N. pachyderma* fluxes and abundance values are like the previous ecozone.

4.3.4 Foraminiferal association B: 953 ± 214.5–696 ± 75.5 years BP

This FoA is defined by the presence of the agglutinated taxa, *P. antarctica* and *P. bartrami*. The upper limit of this FoA is defined by the disappearance of these two species. *M. arenacea* appears sporadically during this period. During this

Table 3. Principal component analysis (PCA) score results and variance explained: *G. biora* FA (PC 1), with a score of 4.4825, explaining 63.42 % of the variance, and *P. antarctica* and *P. bartrami* FA (PC 2), with a score of 2.4112 and 3.6695 respectively, explaining 22.8 % of the variance. These two PCs combined explain 86.22 % of the total variance. Boldface is used to highlight the higher correlation values between the PC and the species.

Species	*G. biora* FA	*P. antarctica*/ *P. bartrami* FA
Astrononion echolsi	−0.32105	−0.33251
Astrononion antarcticus	−0.31377	−0.33024
Cassidulinoides porrectus	−0.32555	−0.33426
Cibicides refulgens	−0.30989	−0.34269
Epistominella exigua	−0.31052	−0.34095
Globocassidulina biora	**4.4825**	−0.69931
Globocassidulina crassa	−0.30673	−0.34239
Globocassidulina sp.	−0.26571	−0.35697
Globocassidulina subglobosa	0.36126	−0.46237
Nonionella bradii	−0.3103	−0.34029
Nonionella iridea	−0.30167	−0.33575
Rosalina globularis	−0.31457	−0.32492
Stainforthia feylingi	−0.22524	−0.34034
Trifarina angulosa	−0.24501	−0.31294
Pyrgo depressa	−0.3278	−0.33573
Labrospira jeffreysii	0.030279	0.51134
Miliammina arenacea	−0.24641	−0.08418
Paratrochammina bartrami	0.30761	**3.6695**
Paratrochammina tricamerata	−0.32386	−0.27074
Portatrochammina antarctica	0.21473	**2.4112**
Portatrochammina bipolaris	−0.32124	−0.3231
Paratrochammina nana	−0.29692	−0.07115
Rhumblerella sp.	−0.33013	−0.31116
Variance explained	63.42	22.8

FoA, the fluxes of *P. antarctica* and *P. bartrami* are comparable with the previous ones, since the abundances of the two agglutinant species increase towards the end of this FoA (Fig. 6), where they abruptly decrease. *N. pachyderma* is absent throughout the interval.

4.3.5 Foraminiferal association A: 696 ± 75.5 years BP to present

This FoA is characterized by the lowest value of accumulation fluxes of every species analysed, with values near zero. The bottom of this FoA coincides with the change in the sedimentation rate (~ 0.5 to $\sim 0.07\,\mathrm{cm\,yr^{-1}}$). This interval is characterized by a very low concentration of specimens (Fig. 4a), making it difficult to interpret relative to microfaunal shift.

5 Discussion

5.1 Edisto Inlet during the Late Holocene

During the austral winter, the Edisto Inlet is generally completely covered by the sea ice. On the other hand, during the austral summer, the fjord is characterized by complete or partial melting of the ice cover. This seasonality leads to a domination of the sedimentation signal from the warmer season compared to the colder one (Tesi et al., 2020). To reconstruct the paleoenvironment evolution of this inlet, we compared our results with those of the previous studied cores in the same region (e.g. core HLF17-1, Tesi et al., 2020; core BAY-50c, Mezgec et al., 2017). The analyses on the HLF17-1 laminae (Tesi et al., 2020) revealed the presence of two clusters, based on the biomarker $IPSO_{25}$ (Ice Proxy for the Southern Ocean with 25 carbon atoms, Belt et al., 2016) and the $\delta^{13}C$, that reflect two different periods over summer, indicative of early fast-ice thawing and protracted opening of the fjord. The threshold that separates the two clusters is used in this study for comparison with the foraminiferal data. In addition, by comparing the results from the foraminiferal assemblage of the TR17-08, from the geochemical proxies of the HLF17-1, and from the diatoms assemblages derived from the BAY05-20 (Megzec et al., 2017), we were able to identify three distinct environmental phases, each characterized by different local sea-ice coverage, environmental conditions and dominant FoA in the Edisto Inlet (Fig. 8).

Table 4. Benthic and planktic foraminiferal species used to define the faunal associations along the studied section of the TR17-08. Here, the name of the species and their ecological features are reported.

Species	Ecology	References
Epistominella exigua	Opportunistic; phytodetritivorous; seasonal fluxes of organic matter; CDW indicator	Mackensen et al. (1990), Gooday (1993), Sabbatini et al. (2004), Ishman and Szymcek (2013), Majewski et al. (2016)
Globocassidulina biora	High hydrodynamism; high bottom current velocity; high sedimentation rate; sub-ice shelf environment	Bernhard (1993), Li et al. (2000), Sabbatini et al. (2004), Ishman and Szymcek (2013), Majewski et al. (2016), Melis and Salvi (2020)
Globocassidulina subglobosa	Opportunistic in response to elevated fluxes of organic carbon; grounding zone wedge foreset	Harloff and Mackensen (1997), Kyrmanidou et al. (2018), Majewski et al. (2020)
Nonionella iridea	Opportunistic; thrives after algal bloom; sensitivity to physical stress	Mackensen et al. (1990), Murray (1991), Gooday (1993), Duffield et al. (2015)
Stainforthia feylingi	Opportunistic; thrives after sea-ice breaks up; low-oxygen environment	Knudsen et al. (2008), Seidenkrantz (2013), Seidenstein et al. (2018)
Trifarina angulosa	High hydrodynamism; high bottom current velocity	Melis and Salvi (2009), Ishman and Szymcek (2013)
Miliammina arenacea	Agglutinated; cold species; high salinity; dissolution condition indicator	Murray (1991), Li et al. (2000), Ishman and Sperling (2002), Ishman and Szymcek (2013), Majewski et al. (2018)
Paratrochammina bartrami	Agglutinated; cold species; sea-ice indicator; low-energy environment	Anderson (1975), Violanti (2000), Majewski and Anderson (2009), Kyrmanidou et al. (2018)
Portatrochammina antarctica	Agglutinated; cold species; low-energy environment; dissolution condition indicator	Anderson (1975), Bernhard (1993), Violanti (2000), Majewski and Anderson (2009), Rodrigues et al. (2010), Majewski et al. (2016), Kyrmanidou et al. (2018)
Neogloboquadrina pachyderma	Planktic species; polar species	Bergami et al. (2009), Schiebel and Hemleben (2017), Mikis et al. (2019), Melis et al. (2021)

5.1.1 Seasonal phase: 2012–1486 years BP

This interval corresponds to the FoA E in the core TR17-08 (Fig. 8). During this period, *Globocassidulina biora* and *G. subglobosa* are the two dominant species and, together with the presence of *Trifarina angulosa*, suggest a well-oxygenated environment with a high bottom current velocity (Mackensen et al., 1990; Li et al., 2000; Melis and Salvi, 2009; Ishman and Szymcek, 2013; Majewski et al., 2018; Capotondi et al., 2020). The dominance of *G. biora* is also represented by the presence of the *G.biora* FA throughout this interval (Fig. 5). Opportunistic species, such as *Nonionella iridea* and *Epistominella exigua*, indicate a high flux of fresh organic matter to the bottom, resulting from algal blooms during the austral summer in response to the break-up of the sea-ice cover (Mackensen et al., 1990; Gooday, 1993; Sabbatini et al., 2004; Majewski et al., 2016; Kyrmanidou et al., 2018). In addition to that, even if in very low concentration, *E. exigua* might suggest the influence of the mCDW in the fjord and the presence of meltwater fluxes (Majewski and Anderson, 2009; Majewski, 2010). The values of the fluxes of *Neogloboquadrina pachyderma* and the BFAR index corroborate the high primary productivity of this period (Peck et al., 2015). During this time interval, in core HLF17-1, the values of $IPSO_{25}$ and $\delta^{13}C$ are frequently lower than the threshold values, indicating ice-free conditions during the austral summers (Fig. 8a, b). The diatom assemblages from core BAY05-20 gives further support of these events. *Fragilariopsis curta*, which is one of the most used sea-ice indicator species (Levanter, 1998), shows relatively low abundances during this period (Mezgec et al., 2017). On the contrary, *Thalassiosira antarctica*, which indicates ice-free conditions (Levanter, 1998), has an average relative abundance that is higher than the other two phases (Mezgec et al., 2017). We suggest that this period corresponds to the presence of a seasonal sea-ice cover, perhaps associated with an intrusion of mCDW along with high primary productivity.

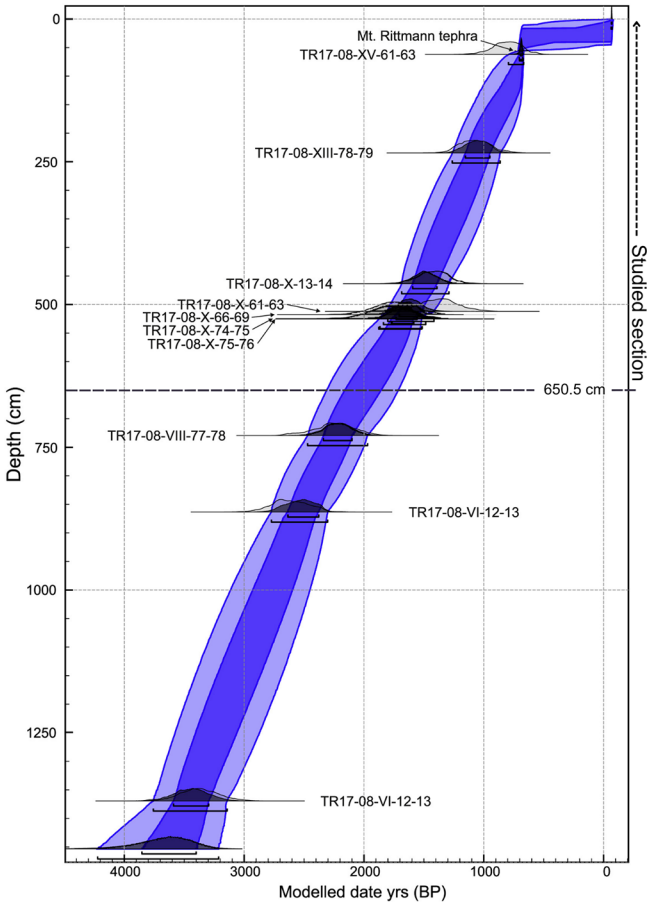

Figure 3. Age–depth model of the TR17-08, calibrated with the Marine 13 curve (adapted from Di Roberto et al., 2023). The studied section is highlighted by the dashed line, as well as the bottom limit of this study (650.5 cm). Dark blue corresponds to the 65 % confidence interval and light blue the 95 % confidence interval.

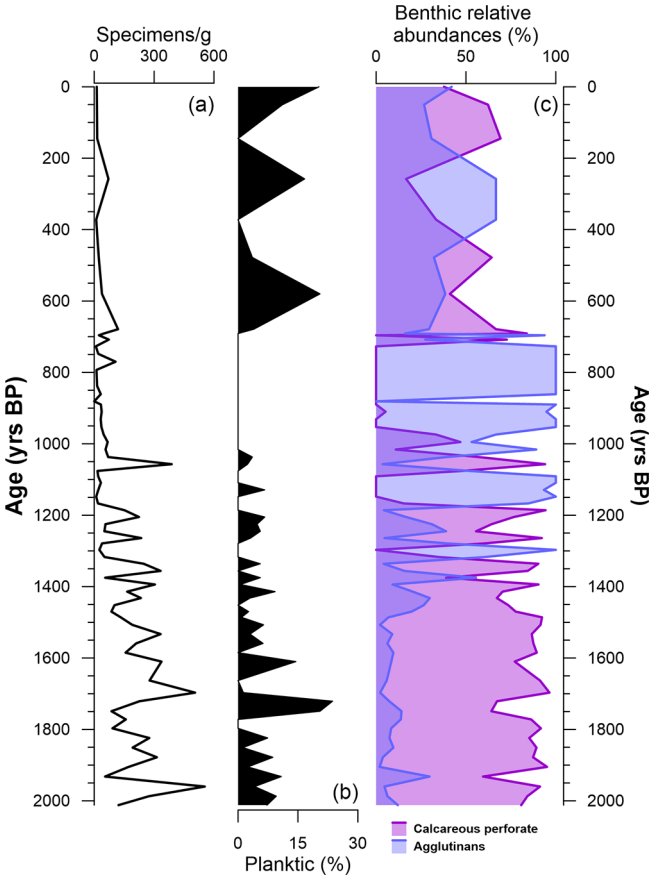

Figure 4. **(a)** Concentration of tests (specimens g^{-1}) along the depth of the studied section (black line). **(b)** Abundance (% of the total specimens; dark area) of planktic species (only *Neogloboquadrina pachyderma*) against depth. **(c)** Relative abundances (% of the total benthic specimens) divided by their test characteristic: calcareous perforate (purple), agglutinated (blue area) against depth.

5.1.2 Transitional phase: 1486–696 years BP

This phase comprehends the FoA D, C and B of the TR17-08 (Fig. 8). The onset of this phase, corresponding to the FoA D, is marked by a sharp increase in accumulation fluxes of the calcareous *Stainforthia feylingi* and the agglutinated *Miliammina arenacea* (Fig. 8f). *Stainforthia feylingi* is a species that thrives in environments with high primary productivity and low oxygen concentrations, indicating a more stratified water column, with lower bottom current velocity, but still affected by the seasonality of the sea-ice cover (Knudsen et al., 2008; Seidenkrantz, 2013; Seidenstein et al., 2018). The presence of *M. arenacea* indicates a high dissolution condition of the carbonate that could have been caused by an increase in residence time of the water masses, by an intrusion of cold and saltier water masses, or by an increase in the organic matter fluxes (Murray, 1991; Li et al., 2000; Ishman and Szymcek, 2013; Majewski et al., 2018). This enhanced dissolution condition is also indicated by the gradual increase in relative abundances of *Paratrochammina bartrami* and *Portatrochammina antarctica* (Fig. 8e). This shift in dominance is also documented by the PCA results, where loadings of the *P. antarctica*/*P. bartrami* FA are significant (Fig. 5). These two agglutinant species with fragile tests indicate a lower-energy environment, with low bottom current velocity, which agrees with longer residence time of the water masses (Anderson, 1975; Majewski and Anderson, 2009; Majewski and Pawlowski, 2010; Rodrigues et al., 2010; Capotondi et al., 2020). Further support of the enhanced dissolution conditions is the abrupt reduction of the accumulation fluxes of *Globocassidulina subglobosa* (Fig. 6). This species is characterized by smaller and thinner tests than *G. biora*, making it more susceptible to dissolution conditions (Bernhard, 1993; Harloff and Mackensen, 1997; Sabbatini et al., 2004). During the FoA D, the BFAR has comparable values with the previous phase, and the loss of opportunistic, phytodetritivorous species (*N. iridea* and *E. exigua*) also suggests an anoxic environment with bottom dissolution conditions (Fig. 8d, g).

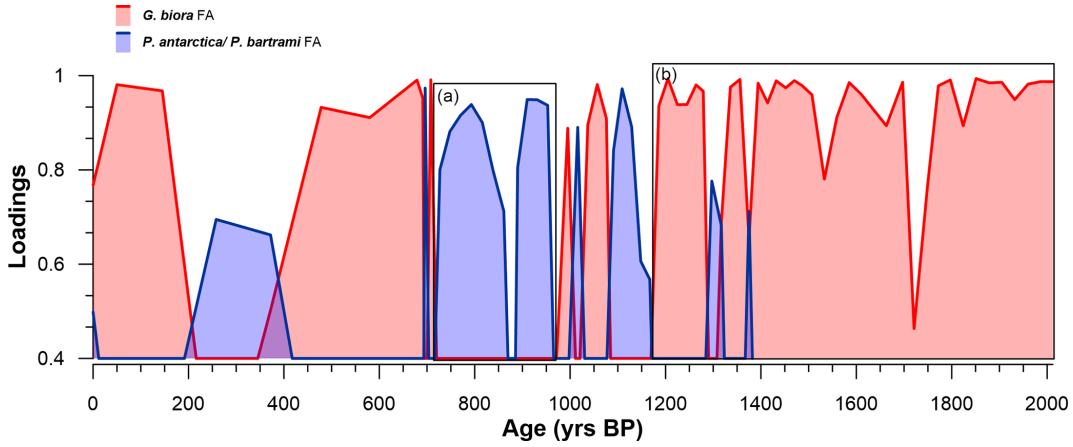

Figure 5. Distribution of the loadings of the two principal axes along the studied section: *G. biora* FA (red-shaded area) and *P. antarctica*/*P. bartrami* FA (blue-shaded area). Only the significant loading values (> 0.4) are displayed. The squares *a* and *b* represent almost continuous periods of above-significance values. Notice that the period from 700 years BP to present has very low resolution with respect to the previous interval (2012–700 years BP).

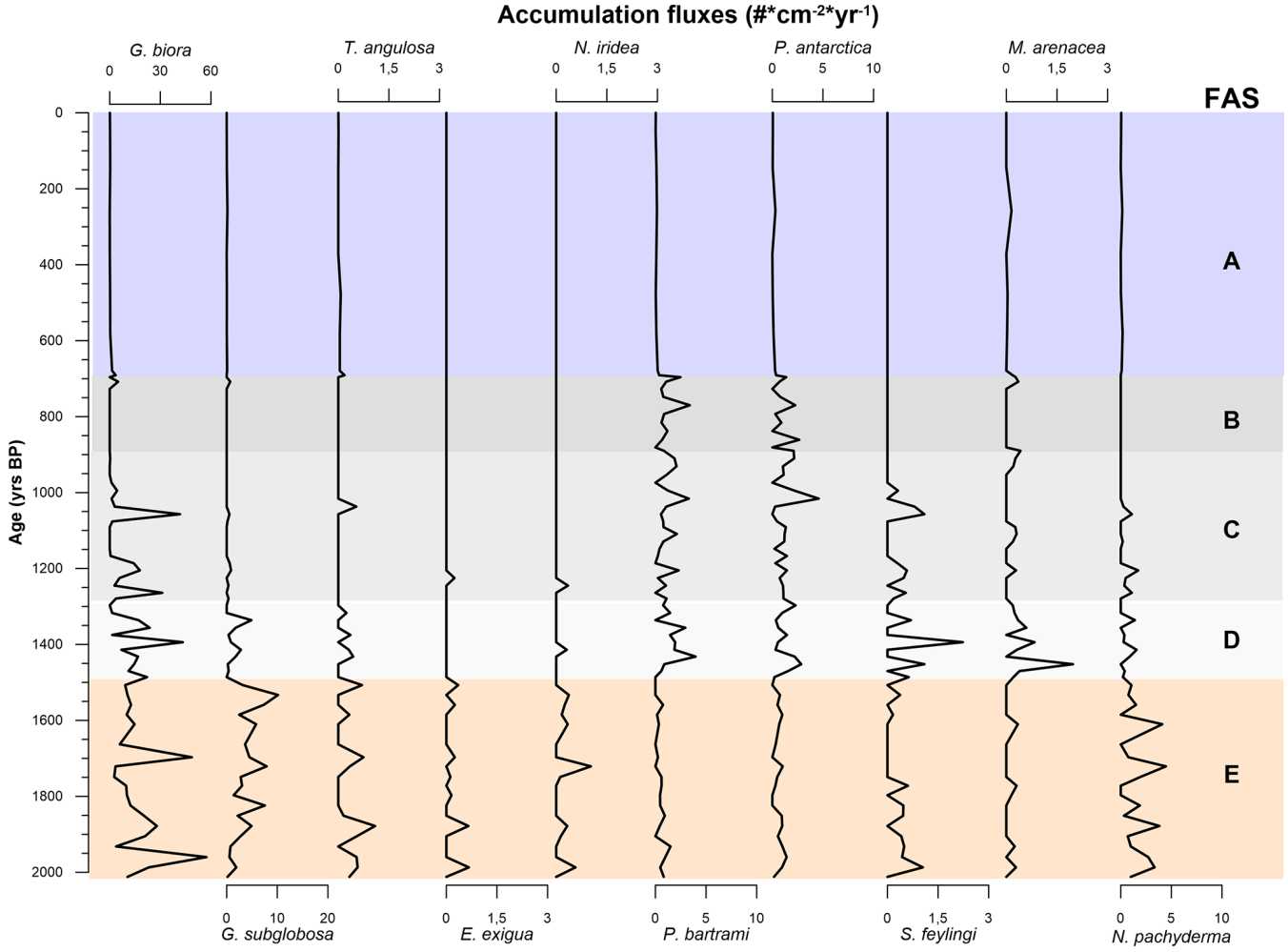

Figure 6. Graphic of the accumulation fluxes of the benthic and planktic species of foraminifera specified in Table 4 over the last 2000 years BP. Graphs are scaled differently from species to species. The FoAs discussed in Sect. 4.3 are highlighted in different colour bands.

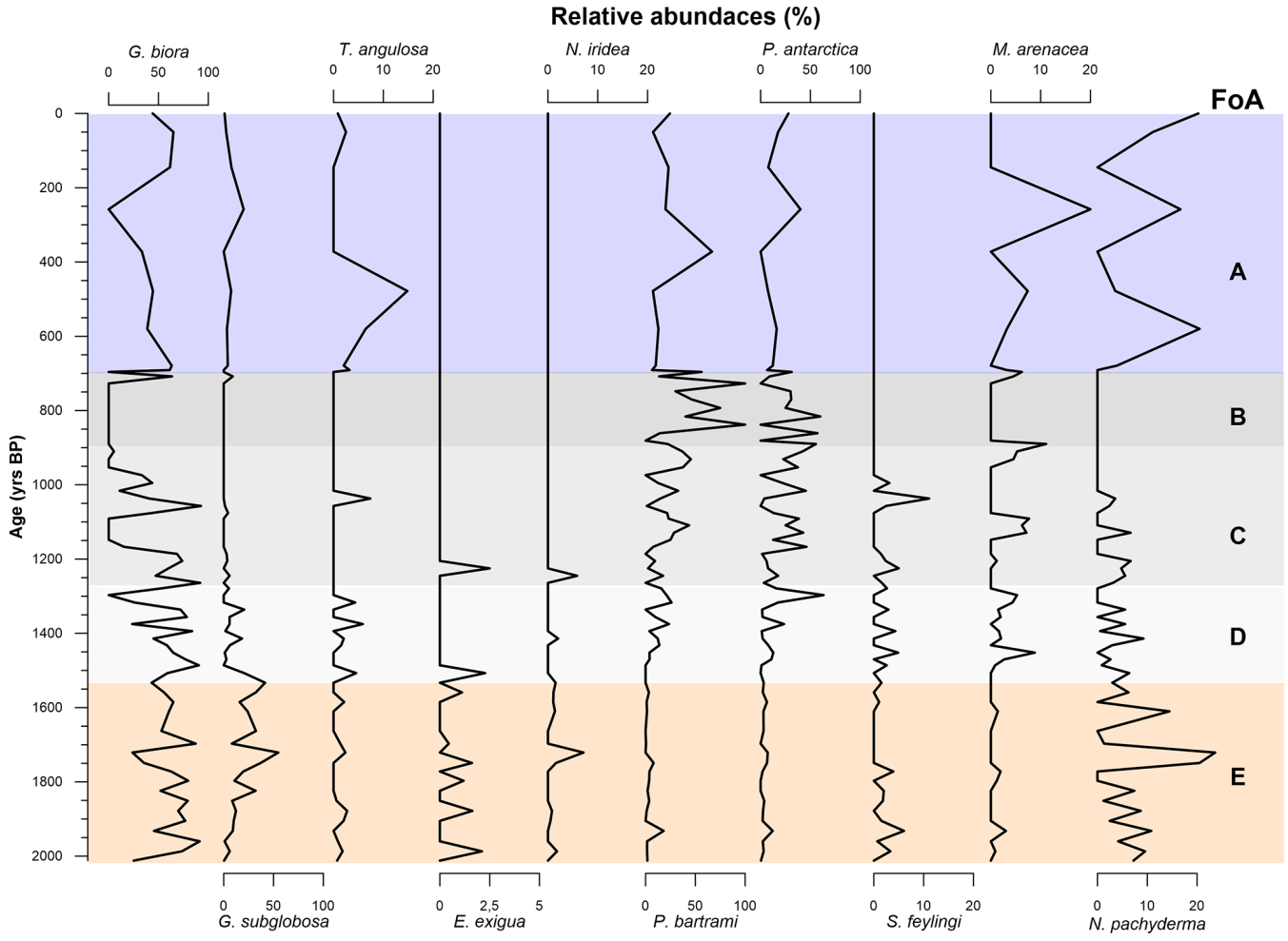

Figure 7. Graphic of relative abundances benthic and planktic species of foraminifera specified in Table 4 over the last 2000 years BP. Graphs are scaled differently from species to species. The FoAs discussed in Sect. 4.3 are highlighted in different colour bands.

During the first period of the transitional phase, the $IPSO_{25}$ and $\delta^{13}C$, from the nearby core HLF17-1, show that the fjord still experiences seasonality of the sea-ice cover, and the diatom assemblages from the core BAY05-20 support that view, with the lowest abundances of *F. curta* and the highest abundances of the *T. antarctica* (Mezgec et al., 2017; Tesi et al., 2020). We speculate that this environment, characterized by oxygen-poor bottom water, high primary productivity and increase of carbonate dissolution, is a consequence of an input of fresh water, probably derived from the retreat of in situ glaciers. Increased freshwater fluxes provide nutrients and enhance thermohaline circulation in fjords, but if the flux values are too high, the water column could become stratified. This could lead to a shutdown of the current local circulation, eventually isolating the fjords from the general circulation, enhancing the stratification of the water column, the development of anoxic conditions and the dissolution of carbonate (Howe et al., 2010; Pan et al., 2020). Since we have no information about the behaviour of the local glaciers in this area during this period, our inference should be regarded as a hypothesis, and local glaciological studies must be addressed to disentangle the complexity of this period.

After the hypothesized glacial discharge event, the second period of this transitional phase (FoA C and FoA B; Fig. 8) shows a gradual transformation of the fjord. The sharp increase in the accumulation fluxes of *S. feylingi* and *M. arenacea* of the FoA D is followed by lower accumulation fluxes and discontinued presence (Fig. 8f). The BFAR gradually goes to near-zero values, along with the *N. pachyderma* accumulation fluxes, which is indicative of a gradual reduction of the primary productivity (Peck et al., 2015). Prolonged periods of water column stratification and lower salinity reduce the vertical mixing of the water masses, reducing the input of nutrients and, consequently, affecting the phytoplankton community (Carvalho et al., 2016) . This can explain the gradual loss of primary productivity after the freshwater pulse, indicated by the BFAR and the *N. pachyderma* fluxes (Hernando et al., 2015; Rozema et al., 2017; Pan et al.,

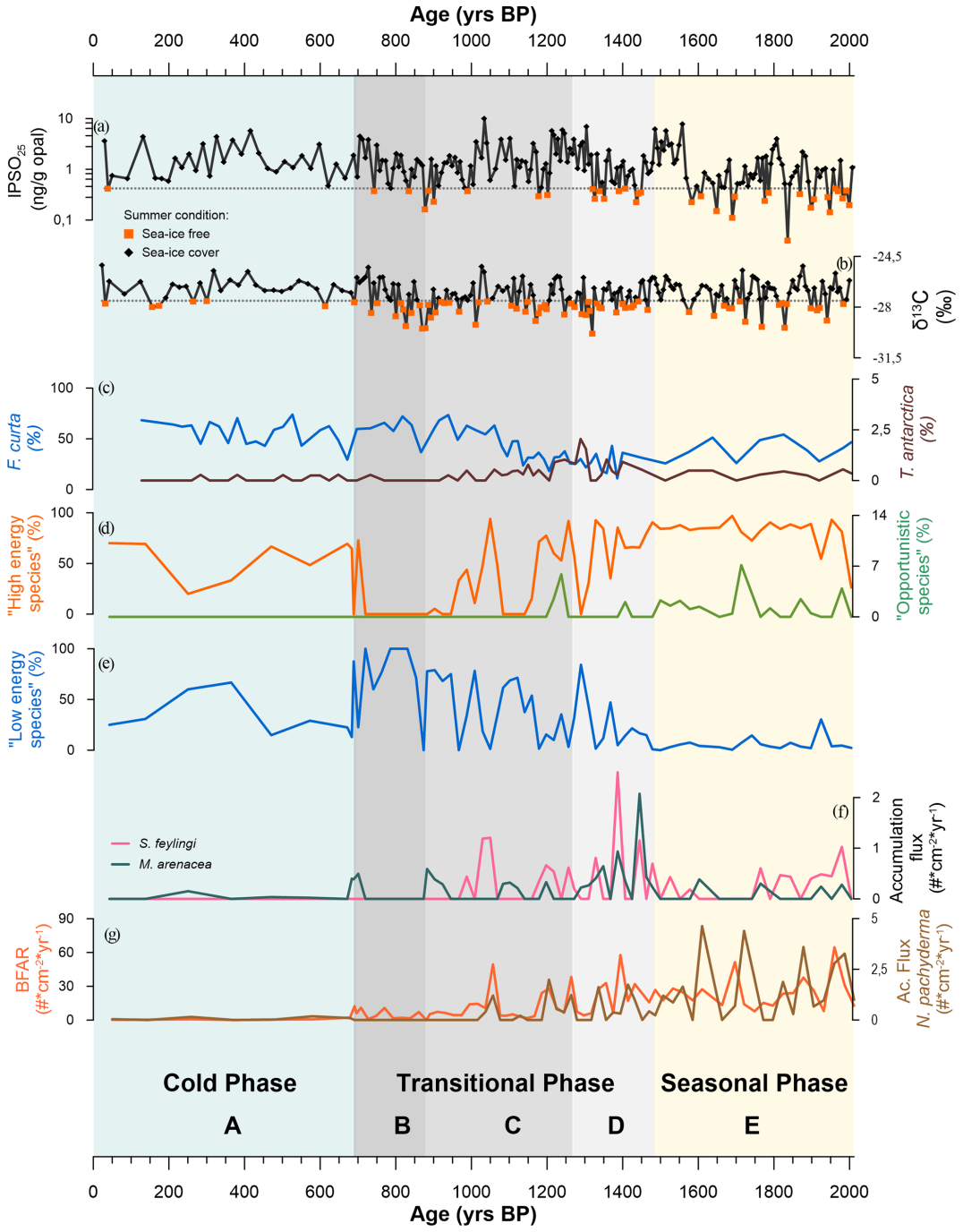

Figure 8. Reconstruction over the last 2000 years of Edisto Inlet. **(a)** $IPSO_{25}$ (ng g^{-1} opal) values (in black) and threshold value (0.42 ng g^{-1}, grey dotted line; orange squares indicate the values below the threshold). Values below the threshold indicate an ice-free inlet during the summer (HLF17-01; Tesi et al., 2020). **(b)** $\delta^{13}C$ values (in black) and the threshold value (−27.56 ‰, grey dotted line; orange squares indicate the value below the threshold). Values below the threshold indicate an ice-free inlet during the summer (HLF17-01; Tesi et al., 2020). **(c)** Relative abundances (%) of the diatoms *Fragilariopsis curta* (dark blue) and *Thalassiosira antarctica* (dark brown) from the WRS_CH core (Mezgec et al., 2017). **(d)** Relative abundances (% of the total benthic specimens) of the benthic assemblage "high-energy species" (*Globocassidulina biora, G. subglobosa* and *Trifarina angulosa*; orange line) and the "opportunistic species" (*Nonionella iridea* and *Epistominella exigua*; green line) from this study. **(e)** Relative abundance (% of the total benthonic specimens) of the low-energy species (*Portatrochammina antarctica* and *Paratrochammina bartrami*; blue line). **(f)** Accumulation fluxes (individuals (#) cm^{-2} yr^{-1}) of *Stainforthia feylingi* (pink) and *Miliammina arenacea* (grey). **(g)** Accumulation fluxes (individuals (#) cm^{-2} yr^{-1}) of the total benthic foraminifera (BFAR, orange line) and of *Neogloboquadrina pachyderma* (dark-brown line). The three phases and the relative foraminiferal association (Sect. 4.3) are also reported: seasonal phase (2014–1472 years BP; light-orange band), transitional phase (1472–700 years BP; grey band) and cold phase (700 years BP to recent; light-blue band).

2020). In addition to that, the presence of freshwater could affect the sea-ice extent positively, as displayed by Pauling et al. (2017). During this period, the foraminiferal assemblage gradually shifts from a *G. biora*-dominated environment, with the presence of calcareous species, to a *P. antarctica*- and *P. bartrami*-dominated environment, at ∼ 900 years BP, suggesting a complete transition from a high-energy environment to a lower-energy environment with higher carbonate dissolution (Fig. 8d, e). The $IPSO_{25}$ and $\delta^{13}C$ from this period display a similar pattern to the previous period but with a frequently lower value below the threshold for the $IPSO_{25}$ index and a positive trend going to the top of the core (Tesi et al., 2020). This positive trend can be explained by the increase in the relative abundance of *F. curta* registered by Megzec et al. (2017), indicating more persistent sea-ice conditions during the second half of this phase (1100–700 years BP). The abrupt increase in the *F. curta* at ∼ 1100 years BP is followed by the shift of the foraminiferal assemblage, from a high-energy environment to a low-energy one (∼ 900 years BP), confirming the view of a sea-ice cover that stays for longer than the cold season, and eventually breaking-up later in the warmer season, or a partial thaw of it during the warmer season (Fig. 8c).

5.1.3 Cold phase: 696 years BP to recent

This last phase corresponds to the FoA A from the core TR17-08 record (Fig. 8). Along this section, there is an almost complete absence of foraminiferal tests, with very low concentration and low accumulation fluxes. The sedimentation rate during this period is almost 1 order of magnitude lower than the previous phase, from an average of 0.49 to $0.07\,cm\,yr^{-1}$ (Fig. 3). The low sedimentation rate could also explain the low fluxes of tests found during this period, since the accumulation flux is a function of the sedimentation rate (Herguera and Berger, 1991). The values of the $IPSO_{25}$ and of the $\delta^{13}C$ are constantly higher than the threshold value, indicating persisting sea-ice conditions during the year (Tesi et al., 2020). The same type of interpretation could be reached by looking at the relative abundances of *F. curta* from the core BAY05-20, which has the highest relative abundances, compared to the two previous phases (Mezgec et al., 2017). In summary, the fjord has experienced a nearly complete loss of seasonality, during this cold phase, with a sea-ice cover formed during the winters but without significant melting or very incipient ones during the warmer seasons, leading to a general very low sedimentation rate and low primary productivity.

5.2 Comparison with other Holocene studies in Antarctica

During the last decade, a series of studies and reviews concerning the last 2000 years of Antarctica regions have been conducted, from ice core data to marine and lacustrine sediment cores, using different proxies, from micropaleontological analyses to geochemical ones. In the last 2000 years, in Antarctica, a major cooling trend has been identified (Stenni et al., 2017) with two major climate phases observed: the Medieval Climate Anomaly (MCA), a warm period spanning from 1700 to 950 years BP (Bertler et al., 2018; Lüning et al., 2019), and the Little Ice Age (LIA), a cold interval from 1100 to 450 years BP (Stenni et al., 2017; Bertler et al., 2018). Both climatic phases are well studied in the Northern Hemisphere, where they were first defined (Matthews and Briffa, 2005; Diaz et al., 2011). The Ross Sea during the MCA seems to have experienced a different climate. Specifically, the climate was relatively warmer than present, although the onset of this warmer condition varies from site to site, as a result of local factors (Mezgec et al., 2017; Bertler et al., 2018; Lüning et al., 2019; Tesi et al., 2020). Throughout the Victoria Land coast, abandoned penguin colonies show the presence of a warmer period during the MCA, along with ice and marine cores (Lüning et al., 2019; Emslie, 2020). At Edmonson Point, Baroni and Orombelli (1994) showed the presence of glacial retreat at 1030–900 years BP, suggesting a warm phase. Jin et al. (2021) analysed the grain size of lacustrine sediments from Inexpressible Island and identify a period of warmer conditions that started at ∼ 1400 years BP. The presence of a warmer period during the MCA was also found in Bunger Hills lacustrine sediments and other lake sediments, with the onset of warmer conditions between 2000 and 1500 years BP (Giralt et al., 2020). Although there is a lack of studies in the Edisto Inlet, we can put forward the hypothesis that a glacial retreat occurred during the MCA in agreement with other studies conducted on the Victoria Land coast around 1400 years BP. The release of large amount of glacier meltwater in the water column can be explained by the presence of three main glaciers, which can release large amounts of freshwater in a very short time and could potentially influence the input and output of the water masses in the Edisto Inlet. The other major climate change event is the LIA, which is well documented throughout Victoria Land by abandoned penguin colonies. Baroni and Orombelli (1994) had already noticed an advance of the Edmonson point glacier during 550–450 years BP, which agrees with the LIA, defined by Hall and Denton (2002), who reported a glacial advance of the Wilson Piedmont Glacier (Scott Coast). Rhodes et al. (2012), studying the glaciochemical proxies from the Ross Sea, concluded that the temperature was lower by $1.6 \pm 0.4\,°C$ compared to the average temperature prior to 100 years BP. This overall cooling of the Ross Sea region during the LIA enhanced the glacial conditions, with larger-than-present sea-ice extent and duration (Bertler et al., 2018). This general cooling during the LIA could explain the drop of the sedimentation rate at ∼ 700 years BP with the increase of the sea-ice cover duration, also observed in the core studied by Tesi et al. (2020).

6 Conclusions

Based on benthic foraminiferal content from the marine sediment core TR17-08 in the Edisto Inlet, we identify five different faunal associations during the last 2000 years BP. Comparison of our results with those of Tesi et al. (2020) and Megzec et al. (2017) demonstrates a general loss of cyclic seasonal behaviour of the sea-ice cover. In summary, three different phases were identified:

- *Seasonal phase* (from 2012–1486 years BP). During this period, Edisto Inlet experienced a seasonal sea-ice cover as indicated by the presence of high-energy species (*Globocassidulina* spp. and *Trifarina angulosa*) and phytodetritivorous species, such as *Nonionella iridea* and *Epistominella exigua*. The presence of *E. exigua* may suggest the intrusion of warm water masses (mCDW) inside the fjord, indicating that it is not isolated from the general oceanic circulation. The low abundances of the diatom *Fragilariopsis curta* (indicative of sea-ice conditions) and more-frequent below-threshold values of $IPSO_{25}$ and $\delta^{13}C$ are in good agreement with this view.

- *Transitional phase* (from 1486–696 years BP). During this period, Edisto Inlet experienced a higher freshwater input, which could be caused by the retreat of the in situ glaciers. More stratified water columns lead to oxygen-poor conditions and higher carbonate dissolution, along with the isolation of the fjord from the general water circulation. Foraminiferal associations show a gradual change: from the high-energy environment with high bottom current velocity to a low-energy environment indicated by the dominance of the agglutinated species (*Portatrochammina antarctica*, *Paratrochammina bartrami* and *M. arenacea*). The increase of *F. curta* at 1.1 kyr BP and the gradual increase of the $IPSO_{25}$ suggest the presence of a seasonal sea-ice cover with prolonged permanence or partial thaws during the warmer seasons in the second period of this phase.

- *Cold phase* (from 696 years BP to present day). During this period, Edisto Inlet experienced a permanent sea-ice cover that did not thaw during the warmer seasons as evidenced by the almost complete absence of foraminifera. This also caused an abrupt decrease in the sedimentation rate by 1 order of magnitude than in other phases. The high abundance of *F. curta*, the always above-threshold values of the $IPSO_{25}$ and $\delta^{13}C$ support this view.

By comparison with other studies in Victoria Land, we were able to recognize the presence of two climate change events: the Medieval Climate Anomaly period, $\sim$ 1400 years BP, indicated by the freshwater pulse at the start of the transitional phase, and the Little Ice Age, a colder period, $\sim$ 680 years BP, indicated by the absence of foraminifera and the abrupt drop of the sedimentation rate. The different timings of these two climate change events, with respect to other Victoria Land Coast studies, suggest the presence of a local influence of the climate signals.

Appendix A: SEM photos of foraminifera species listed in Table 4.

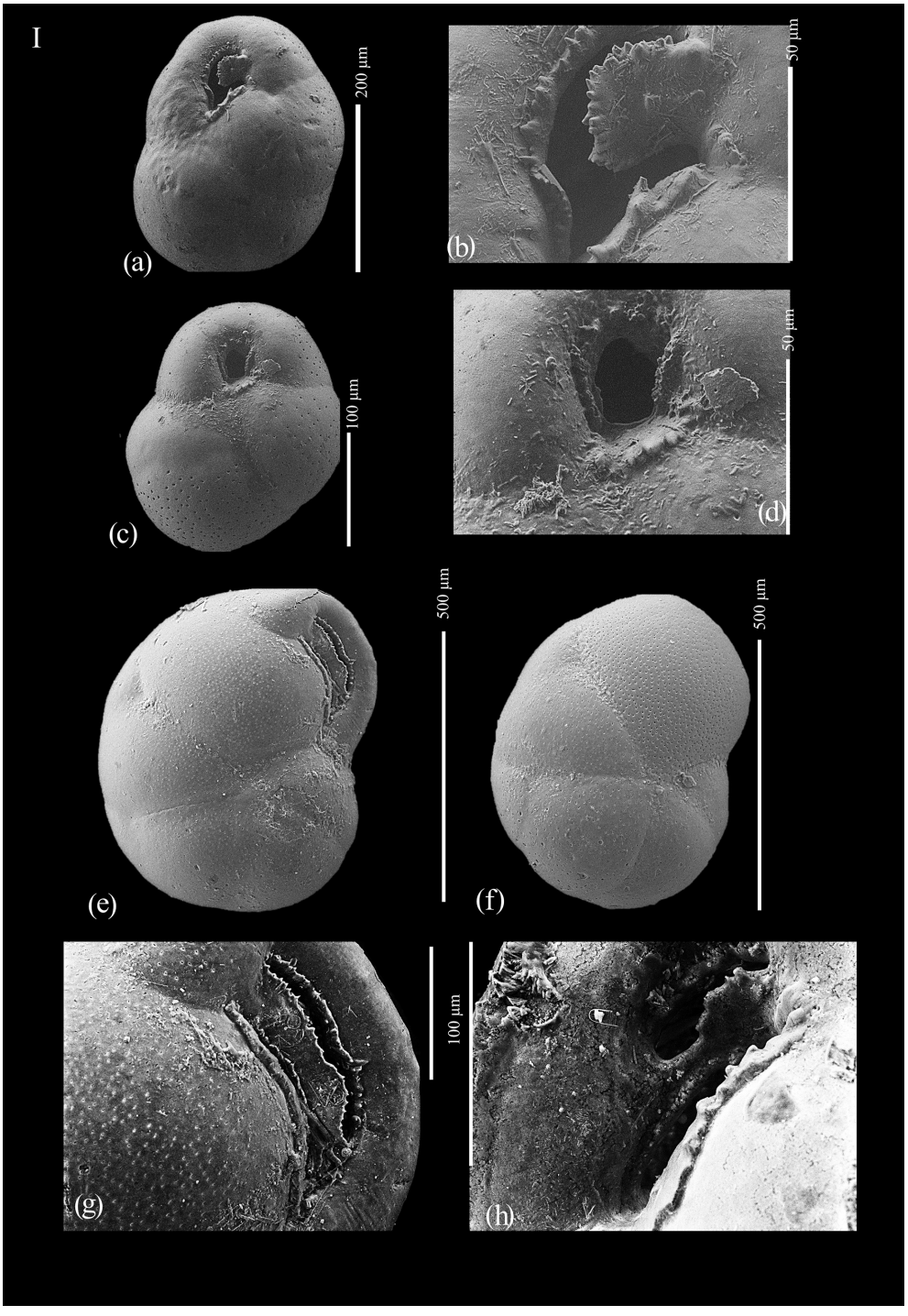

Figure A1. **(a)** *Globocassidulina biora*, juvenile; **(b)** aperture of juvenile *Globocassidulina biora*; **(c)** *Globocassidulina subglobosa*; **(d)** aperture of *Globocassidulina subglobosa*; **(e)** *Globocassidulina biora*, adult, ventral view; **(f)** *Globocassidulina biora*, adult, dorsal view; **(g)** detail of the aperture of an adult of *G. biora*; and **(h)** detail of the aperture of an adult of *G. biora*.

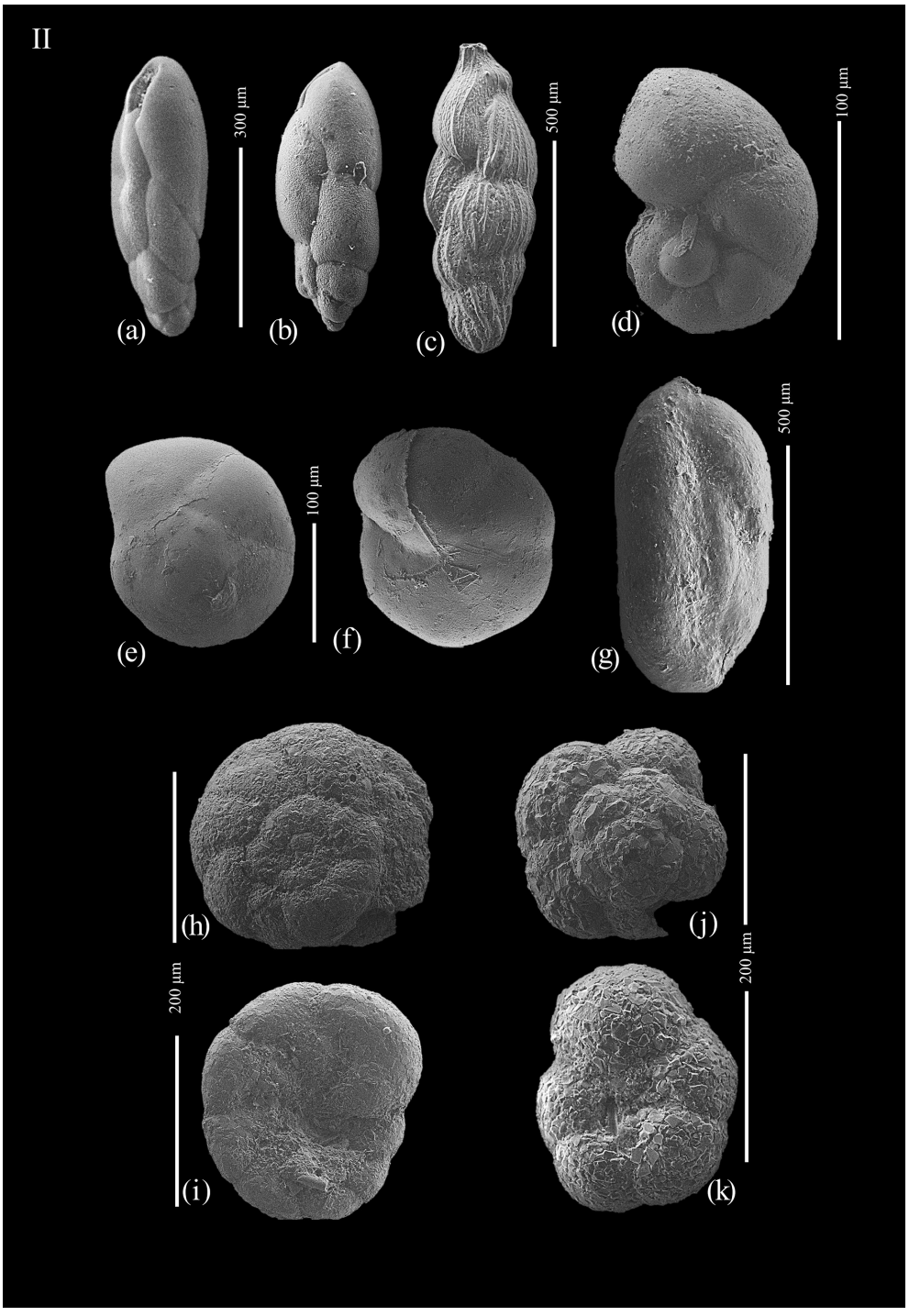

Figure A2. **(a)** *Stainforthia feylingi*; **(b)** *Stainforthia feylingi*; **(c)** *Trifarina angulosa*; **(d)** *Nonionella iridea*; **(e)** *Epistominella exigua*, dorsal view; **(f)** *Epistominella exigua*, ventral view; **(g)** *Miliammina arenacea*; **(h)** *Paratrochammina bartrami*, dorsal view; **(i)** *Paratrochammina bartrami*, ventral view; **(j)** *Portatrochammina antarctica*, dorsal view; and **(k)** *Portatrochammina antarctica*, ventral view.

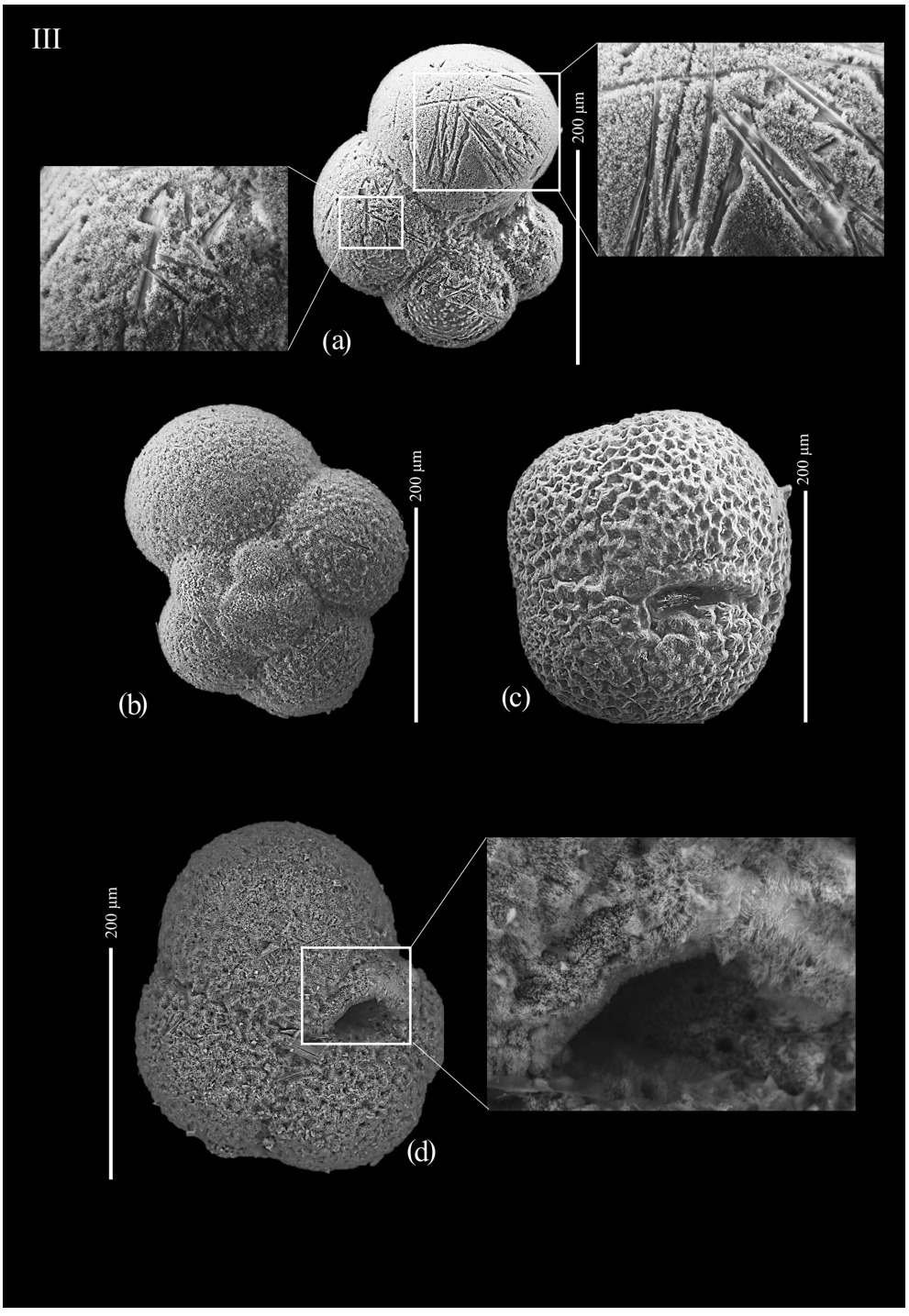

Figure A3. **(a)** *Neogloboquadrina pachyderma*; **(b)** *Neogloboquadrina pachyderma*; **(c)** *Neogloboquadrina pachyderma*; and **(d)** *Neogloboquadrina pachyderma*.

Data availability. All the data used in this study are included the article and in the Supplement.

Supplement. The supplement related to this article is available online at: https://doi.org/10.5194/jm-42-95-2023-supplement.

Author contributions. GG: conceptualization, formal analysis, investigation, visualization, writing the original draft and preparation; CM, KG and RM: supervision, investigation, validation; AG, EC, LL and PG: data curation; ADR and KG: funding acquisition; KG and PG: project administration. All authors contributed to the reviewing and editing process.

Competing interests. The contact author has declared that none of the authors has any competing interests.

Disclaimer. Publisher's note: Copernicus Publications remains neutral with regard to jurisdictional claims in published maps and institutional affiliations.

Special issue statement. This article is part of the special issue "Advances in Antarctic chronology, paleoenvironment, and paleoclimate using microfossils: Results from recent coring campaigns". It is not associated with a conference.

Acknowledgements. We thank the Sorting Centre of MNA – Trieste (Italy) for providing sediment core samples.

Financial support. This research has been supported by the Ministero dell'Università e della Ricerca (projects EDISTHO (grant no. PNRA 2018_00010) and TRACERS (grant no. PNRA2016-A3/00055)).

Review statement. This paper was edited by R. Mark Leckie and reviewed by Samantha Bombard and Scott Ishman.

References

Abdi, H. and Williams, L. J.: Principal component analysis, Wires Comput. Mol. Sci., 2, 433–459, https://doi.org/10.1002/wics.101, 2010.

Ainley, D. G. and Jacobs, S. S.: Sea-bird affinities for ocean and ice boundaries in the Antarctic, Deep-Sea Res. Pt. A, 28, 1173–1185, https://doi.org/10.1016/0198-0149(81)90054-6, 1981.

Anderson, J. B.: Ecology and Distribution of Foraminifera in the Weddel Sea of Antarctica, Micropaleontology, 21, 69–96, https://doi.org/10.2307/1485156, 1975.

Asioli, A. and Langone, L.: Relationship between recent planktic foramnifera and water masses properties in the western Ross Sea (Antarctica), Comitato glaciologico italiano, Bollettino, Ser. 3, Geogr. Fis. Din. Quat., 20, 193–198, 1997.

Baroni, C. and Orombelli, G.: Holocene glacier variations in the Terra Nova Bay area (Victoria Land, Antarctica), Antarct. Sci., 6, 497–505, https://doi.org/10.1017/S0954102094000751, 1994.

Belt, S. T., Smik, L., Brown, T. A., Kim, J. H., Rowland, S. J., Allen, C. S., Gal, J. K., Shin, K. H., Lee, J. I., and Taylor, K. W.: Source identification and distribution reveals the potential of the geochemical Antarctic sea ice proxy IPSO25, Nat. Commun., 7, 12655, https://doi.org/10.1038/ncomms12655, 2016.

Bergami, C., Capotondi, L., Langone, L., Giglio, F., and Ravaioli, M.: Distribution of living planktonic foraminifera in the Ross Sea and the Pacific sector of the Southern Ocean (Antarctica), Mar. Micropaleontol., 73, 37–48, https://doi.org/10.1016/j.marmicro.2009.06.007, 2009.

Bernhard, J. M.: Experimental and field evidence of Antarctic foraminiferal tolerance to anoxia and hydrogen sulfide, Mar. Micropaleontol., 20, 203–213, https://doi.org/10.1016/0377-8398(93)90033-T, 1993.

Bertler, N. A. N., Conway, H., Dahl-Jensen, D., Emanuelsson, D. B., Winstrup, M., Vallelonga, P. T., Lee, J. E., Brook, E. J., Severinghaus, J. P., Fudge, T. J., Keller, E. D., Baisden, W. T., Hindmarsh, R. C. A., Neff, P. D., Blunier, T., Edwards, R., Mayewski, P. A., Kipfstuhl, S., Buizert, C., Canessa, S., Dadic, R., Kjær, H. A., Kurbatov, A., Zhang, D., Waddington, E. D., Baccolo, G., Beers, T., Brightley, H. J., Carter, L., Clemens-Sewall, D., Ciobanu, V. G., Delmonte, B., Eling, L., Ellis, A., Ganesh, S., Golledge, N. R., Haines, S., Handley, M., Hawley, R. L., Hogan, C. M., Johnson, K. M., Korotkikh, E., Lowry, D. P., Mandeno, D., McKay, R. M., Menking, J. A., Naish, T. R., Noerling, C., Ollive, A., Orsi, A., Proemse, B. C., Pyne, A. R., Pyne, R. L., Renwick, J., Scherer, R. P., Semper, S., Simonsen, M., Sneed, S. B., Steig, E. J., Tuohy, A., Venugopal, A. U., Valero-Delgado, F., Venkatesh, J., Wang, F., Wang, S., Winski, D. A., Winton, V. H. L., Whiteford, A., Xiao, C., Yang, J., and Zhang, X.: The Ross Sea Dipole – temperature, snow accumulation and sea ice variability in the Ross Sea region, Antarctica, over the past 2700 years, Clim. Past, 14, 193–214, https://doi.org/10.5194/cp-14-193-2018, 2018.

Brambati, A., Fanzutti, G. P., Finocchiaro, F., Melis, R., Pugliese, N., Salvi, G., and Faranda, C.: Some Palaeoecological Remarks on the Ross Sea Shelf, Antarctica, in: Ross Sea Ecology, edited by: Faranda, F. M., Guglielmo, L., and Ianora, A., Springer, Berlin, Heidelberg, 51–61, https://doi.org/10.1007/978-3-642-59607-0_5, 2000.

Capotondi, L., Bonomo, S., Budillon, G., Giordano, P., and Langone, L.: Living and dead benthic foraminiferal distribution in two areas of the Ross Sea (Antarctica), Rendiconti Lincei, Scienze Fisiche e Naturali, 31, 1037–1053, https://doi.org/10.1007/s12210-020-00949-z, 2020.

Carvalho, F., Kohut, J., Oliver, M. J., Sherrell, R. M., and Schofield, O.: Mixing and phytoplankton dynamics in a submarine canyon in the West Antarctic Peninsula, J. Geophys. Res.-Ocean., 121, 5069–5083, https://doi.org/10.1002/2016jc011650, 2016.

Castagno, P., Falco, P., Dinniman, M. S., Spezie, G., and Budillon, G.: Temporal variability of the Circumpolar Deep Water inflow onto the Ross Sea continental shelf, J. Mar. Syst., 166, 37–49, https://doi.org/10.1016/j.jmarsys.2016.05.006, 2017.

Di Roberto, A., Colizza, E., Del Carlo, P., Petrelli, M., Finocchiaro, F., and Kuhn, G.: First marine cryptotephra in Antarctica found in sediments of the western Ross Sea correlates with englacial tephras and climate records, Sci. Rep., 9, 10628, https://doi.org/10.1038/s41598-019-47188-3, 2019.

Di Roberto, A., Re, G., Scateni, B., Petrelli, M., Tesi, T., Capotondi, L., Morigi, C., Galli, G., Colizza, E., Melis, R., Torricella, F., Giordano, P., Giglio, F., Gallerani, A., and Gariboldi, K.: Cryptotephras in the marine sediment record of the Edisto Inlet, Ross Sea: Implications for the volcanology and tephrochronology of northern Victoria Land, Antarctica, Quaternary Sci. Adv., 10, 100079, https://doi.org/10.1016/j.qsa.2023.100079, 2023.

Diaz, H. F., Trigo, R., Malcolm, H. K., Mann, M. E., Xoplaki, E., and Barriopedro, D.: Spatial and temporal characteristics of climate in medieval times revisited, Bull. Am. Meteorol. Soc., 92, 1487–1500, 2011.

Dotto, T. S., Naveira Garabato, A., Bacon, S., Tsamados, M., Holland, P. R., Hooley, J., et al.: Variability of the Ross Gyre, Southern Ocean: Drivers and responses revealed by satellite altimetry, Geophys. Res. Lett., 45, 6195–6204, https://doi.org/10.1029/2018GL078607, 2018.

Duffield, C. J., Hess, S., Norling, K., and Alve, E.: The response of Nonionella iridea and other benthic foraminifera to "fresh" organic matter enrichment and physical disturbance, Mar. Micropaleontol., 120, 20–30, https://doi.org/10.1016/j.marmicro.2015.08.002, 2015.

Eayrs, C., Holland, D., Francis, D., Wagner, T., Kumar, R., and Li, X.: Understanding the Seasonal Cycle of Antarctic Sea Ice Extent in the Context of Longer-Term Variability, Rev. Geophys., 57, 1037–1064, https://doi.org/10.1029/2018rg000631, 2019.

Emslie, S. D.: Ancient Adélie penguin colony revealed by snowmelt at Cape Irizar, Ross Sea, Antarctica, Geology, 49, 145–149, https://doi.org/10.1130/g48230.1, 2020.

Finocchiaro, F., Langone, L., Colizza, E., Fontolan, G., Giglio, F., and Tuzzi, E.: Record of the early Holocene warming in a laminated sediment core from Cape Hallett Bay (Northern Victoria Land, Antarctica), Glob. Planet. Change, 45, 193–206, https://doi.org/10.1016/j.gloplacha.2004.09.003, 2005.

Fraser, A. D., Massom, R. A., Michael, K. J., Galton-Fenzi, B. K., and Lieser, J. L.: East Antarctic Landfast Sea Ice Distribution and Variability, 2000–08, J. Clim., 25, 1137–1156, https://doi.org/10.1175/jcli-d-10-05032.1, 2012.

Gales, J. A., McKay, R. M., De Santis, L., Rebesco, M., Laberg, J. S., Shevenell, A. E., Harwood, D., Leckie, R. M., Kulhanek, D. K., King, M., Patterson, M., Lucchi, R. G., Kim, S., Kim, S., Dodd, J., Seidenstein, J., Prunella, C., Ferrante, G. M., and Scientists, I. E.: Climate-controlled submarine landslides on the Antarctic continental margin, Nat. Commun., 14, 2714, https://doi.org/10.1038/s41467-023-38240-y, 2023.

Giralt, S., Hernández, A., Pla-Rabes, S., Antoniades, D., Toro, M., Granados, I., and Oliva, M.: Holocene environmental changes inferred from Antarctic lake sediments, Chap. 3, edited by: Oliva, M. and Ruiz-Fernández, J., Past Antarctica, Academic Press, 51–66, https://doi.org/10.1016/b978-0-12-817925-3.00003-3, 2020.

Gooday, A. J.: Deep-sea benthic foraminiferal species which exploit phytodetritus: Characteristic features and controls on distribution, Mar. Micropaleontol., 22, 187–205, https://doi.org/10.1016/0377-8398(93)90043-W, 1993.

Hall, B. L., Denton, G. H., Overturf, B., and Hendy, C. H.: Glacial Lake Victoria, a high-level Antarctic Lake inferred from lacustrine deposits in Victoria Valley, J. Quaternary Sci., 17, 697–706, https://doi.org/10.1002/jqs.691, 2002.

Hammer, O., Harper, D. T. A., and Ryan, P. D.: PAST: Paleontological Statistic Software package for education and data analyses, Palaeontol. Electron., 4, 9 pp., http://palaeo-electronica.org/2001_1/past/issue1_01.htm (last access: 11 August 2023), 2001.

Harloff, J. and Mackensen, A.: Recent benthic foraminiferal associations and ecology of the Scotia Sea and Argentin Basin, Mar. Micropaleontol., 31, 1–29, https://doi.org/10.1016/S0377-8398(96)00059-X, 1997.

Herguera, J. C. and Berger, W. H.: Paleoproductivity from benthic foraminifera abundance: Glacial to postglacial change in the west-equatorial Pacific, Geology, 19, 1173–1176, 1991.

Hernando, M., Schloss, I. R., Malanga, G., Almandoz, G. O., Ferreyra, G. A., Aguiar, M. B., and Puntarulo, S.: Effects of salinity changes on coastal Antarctic phytoplankton physiology and assemblage composition, J. Exp. Mar. Biol. Ecol., 466, 110–119, https://doi.org/10.1016/j.jembe.2015.02.012, 2015.

Hilbrecht, H.: Morphologic gradation and ecology of *Neogloboquadrina pachyderma* and *N. dutertrei* (planktic foraminifera) from top core sediments, Mar. Micropaleontol., 31, 31–43, https://doi.org/10.1016/S0377-8398(96)00054-0, 1997.

Howe, J. A., Austin, W. E. N., Forwick, M., Paetzel, M., Harland, R., and Cage, A. G.: Fjord systems and archives: a review, Geol. Soc. Lond. Spec. Publ., 344, 5–15, https://doi.org/10.1144/sp344.2, 2010.

Igarashi, A., Numanami, H., Tsuchiya, Y., and Fukuchi, M.: Bathymetric distribution of fossil foraminifera within marine sediment cores from the eastern part of Lutzow-Holtz Bay, East Antarctica, and its paleoceanographic implications, Mar. Micropaleontol., 42, 125–162, https://doi.org/10.1016/S0377-8398(01)00004-4, 2001.

Ishman, S. E. and Sperling, M. R.: Benthic foraminiferal record of Holocene deep-water evolution in the Palmer Deep, western Antarctica Peninsula, Geology, 30, 435–438, https://doi.org/10.1130/0091-7613(2002)030<0435:BFROHD>2.0.CO;2, 2002.

Ishman, S. E. and Szymcek, P.: Foraminiferal Distributions in the Former Larsen-A Ice Shelf and Prince Gustav Channel Region, Eastern Antarctic Peninsula Margin: A Baseline for Holocene Paleoenvironmental Change, in: Antarctic Peninsula Climate Variability: Historical and Paleoenvironmental Perspectives, Antarct. Res. Ser., 239–260, https://doi.org/10.1029/AR079p0239, 2013.

Jin, J., Chen, X., Xu, L., Nie, Y., Wang, X., Huang, H., Emslie, S. D., and Liu, X.: Chronology and paleoclimatic implications of lacustrine sediments at Inexpressible Island, Ross Sea, Antarctica, Palaeogeogr. Palaeocl., 576, 110497, https://doi.org/10.1016/j.palaeo.2021.110497, 2021.

Knudsen, K. L., Stabell, B., Seidenkrantz, M.-S., EirÍKsson, J., and Blake, W.: Deglacial and Holocene conditions in northernmost Baffin Bay: sediments, foraminifera, diatoms and stable isotopes, Boreas, 37, 346–376, https://doi.org/10.1111/j.1502-3885.2008.00035.x, 2008.

Kyrmanidou, A., Vadman, K. J., Ishman, S. E., Leventer, A., Brachfeld, S., Domack, E. W., and Wellner, J. S.: Late Holocene oceanographic and climatic variability recorded by the Per-

severance Drift, northwestern Weddell Sea, based on benthic foraminifera and diatoms, Mar. Micropaleontol., 141, 10–22, https://doi.org/10.1016/j.marmicro.2018.03.001, 2018.

Levanter, A.: The fate of antarctic "sea-ice diatoms" and their use as paleoenvironmental indicator, edited by: Lizotte, M. P. and Arrigo, K. R., Antarctic Sea Ice: Biological Processes, Interactions and Variability, Antarctic Research Series, 73, 121–137, https://doi.org/10.1029/AR073p0121, 1998.

Li, B., Yoon, H., and Park, B.: Foraminiferal assemblages and $CaCO_3$ dissolution since the last deglaciation in the Maxwell Bay, King George Island, Antarctica, Mar. Geol., 169, 239–257, https://doi.org/10.1016/S0025-3227(00)00059-1, 2000.

Lüning, S., Gałka, M., and Vahrenholt, F.: The Medieval Climate Anomaly in Antarctica, Palaeogeogr. Palaeocl., 532, 109251, https://doi.org/10.1016/j.palaeo.2019.109251, 2019.

Mackensen, A., Grobe, H., Kuhn, G., and Futterer, D. K.: Benthic foraminiferal assemblages from the eastern Weddell Sea between 68 and 73° S: distribution, ecology and fossilization potential, Mar. Micropaleontol., 16, 241–283, https://doi.org/10.1016/0377-8398(90)90006-8, 1990.

Majewski, W.: Benthic foraminifera from West Antarctic fiord environments: An overview, Polish Pol. Res., 31, 61–82, https://doi.org/10.4202/ppres.2010.05, 2010.

Majewski, W. and Anderson, J. B.: Holocene foraminiferal assemblages from Firth of Tay, Antarctic Peninsula: Paleoclimate implications, Mar. Micropaleontol., 73, 135–147, https://doi.org/10.1016/j.marmicro.2009.08.003, 2009.

Majewski, W. and Pawlowski, J.: Morphologic and molecular diversity of the foraminiferal genus Globocassidulina in Admiralty Bay, King George Island, Antarct. Sci., 22, 271–281, https://doi.org/10.1017/s0954102010000106, 2010.

Majewski, W., Wellner, J. S., and Anderson, J. B.: Environmental connotations of benthic foraminiferal assemblages from coastal West Antarctica, Mar. Micropaleontol., 124, 1–15, https://doi.org/10.1016/j.marmicro.2016.01.002, 2016.

Majewski, W., Bart, P. J., and McGlannan, A. J.: Foraminiferal assemblages from ice-proximal paleo-settings in the Whales Deep Basin, eastern Ross Sea, Antarctica, Palaeogeogr. Palaeocl., 493, 64–81, https://doi.org/10.1016/j.palaeo.2017.12.041, 2018.

Majewski, W., Prothro, L. O., Simkins, L. M., Demianiuk, E. J., and Anderson, J. B.: Foraminiferal Patterns in Deglacial Sediment in the Western Ross Sea, Antarctica: Life Near Grounding Lines, Paleoceanogr. Paleocl., 35, e2019PA003716, https://doi.org/10.1029/2019pa003716, 2020.

Maksym, T.: Arctic and Antarctic Sea Ice Change: Contrasts, Commonalities, and Causes, Ann. Rev. Mar. Sci., 11, 187–213, https://doi.org/10.1146/annurev-marine-010816-060610, 2019.

Malmgren, B. U. and Haq, B. A.: Assessment of quantitative techniques in paleobiogeography, Mar. Micropaleontol., 7, 213–236, https://doi.org/10.1016/0377-8398(82)90003-2, 1982.

Matsuoka, K., Skoglund, A., Roth, G., de Pomereu, J., Griffiths, H., Headland, R., Herried, B., Katsumata, K., Le Brocq, A., Licht, K., Morgan, F., Neff, P. D., Ritz, C., Scheinert, M., Tamura, T., Van de Putte, A., van den Broeke, M., von Deschwanden, A., Deschamps-Berger, C., Van Liefferinge, B., Tronstad, S., and Melvær, Y.: Quantarctica, an integrated mapping environment for Antarctica, the Southern Ocean, and sub-Antarctic islands, Environ. Model. Softw., 140, 105015, https://doi.org/10.1016/j.envsoft.2021.105015, 2021.

Matthews, J. A. and Briffa, K. R.: The "little ice age": Re-evaluation of an evolving concept, Geogr. Ann. A, 87, 17–36, https://doi.org/10.1175/BAMS-D-10-05003.1, 2005.

Meehl, G. A., Teng, H., and Arblaster, J. M.: Climate model simulations of the observed early-2000s hiatus of global warming, Nat. Clim. Change, 4, 898–902, https://doi.org/10.1038/nclimate2357, 2014.

Melis, R. and Salvi, G.: Late Quaternary foraminiferal assemblages from western Ross Sea (Antarctica) in relation to the main glacial and marine lithofacies, Mar. Micropaleontol., 70, 39–53, https://doi.org/10.1016/j.marmicro.2008.10.003, 2009.

Melis, R. and Salvi, G.: Foraminifer and Ostracod Occurrence in a Cool-Water Carbonate Factory of the Cape Adare (Ross Sea, Antarctica): A Key Lecture for the Climatic and Oceanographic Variations in the Last 30,000 Years, Geosciences, 10, 413, https://doi.org/10.3390/geosciences10100413, 2020.

Mezgec, K., Stenni, B., Crosta, X., Masson-Delmotte, V., Baroni, C., Braida, M., Ciardini, V., Colizza, E., Melis, R., Salvatore, M. C., Severi, M., Scarchilli, C., Traversi, R., Udisti, R., and Frezzotti, M.: Holocene sea ice variability driven by wind and polynya efficiency in the Ross Sea, Nat. Commun., 8, 1334, https://doi.org/10.1038/s41467-017-01455-x, 2017.

Mikis, A., Hendry, K. R., Pike, J., Schmidt, D. N., Edgar, K. M., Peck, V., Peeters, F. J. C., Leng, M. J., Meredith, M. P., Jones, C. L. C., Stammerjohn, S., and Ducklow, H.: Temporal variability in foraminiferal morphology and geochemistry at the West Antarctic Peninsula: a sediment trap study, Biogeosciences, 16, 3267–3282, https://doi.org/10.5194/bg-16-3267-2019, 2019.

Murray, J. W.: Ecology and palaeoecology of benthic foraminifera, Routledge, https://doi.org/10.4324/9781315846101, 1991.

Orsi, A. H. and Wiederwohl, C. L.: A recount of Ross Sea waters, Deep-Sea Res. Pt. II, 56, 778–795, https://doi.org/10.1016/j.dsr2.2008.10.033, 2009.

Pan, B. J., Vernet, M., Manck, L., Forsch, K., Ekern, L., Mascioni, M., Barbeau, K. A., Almandoz, G. O., and Orona, A. J.: Environmental drivers of phytoplankton taxonomic composition in an Antarctic fjord, Prog. Oceanogr., 183, 102295, https://doi.org/10.1016/j.pocean.2020.102295, 2020.

Parkinson, C. L. and Cavalieri, D. J.: Antarctic sea ice variability and trends, 1979–2010, The Cryosphere, 6, 871–880, https://doi.org/10.5194/tc-6-871-2012, 2012.

Pauling, A. G., Smith, I. J., Langhorne, P. J., and Bitz, C. M.: Time-Dependent Freshwater Input From Ice Shelves: Impacts on Antarctic Sea Ice and the Southern Ocean in an Earth System Model, Geophys. Res. Lett., 44, 10454–410461, https://doi.org/10.1002/2017gl075017, 2017.

Peck, V. L., Allen, C. S., Kender, S., McClymont, E. L., and Hodgson, D. A.: Oceanographic variability on the West Antarctic Peninsula during the Holocene and the influence of upper circumpolar deep water, Quaternary Sci. Rev., 119, 54–65, https://doi.org/10.1016/j.quascirev.2015.04.002, 2015.

Rhodes, R. H., Bertler, N. A. N., Baker, J. A., Steen-Larsen, H. C., Sneed, S. B., Morgenstern, U., and Johnsen, S. J.: Little Ice Age climate and oceanic conditions of the Ross Sea, Antarctica from a coastal ice core record, Clim. Past, 8, 1223–1238, https://doi.org/10.5194/cp-8-1223-2012, 2012.

Rodrigues, A. R., Maluf, J. C. C., Braga, E. d. S., and Eichler, B. B.: Recent benthic foraminiferal distribution and related environmental factors in Ezcurra Inlet, King

George Island, Antarctica, Antarct. Sci., 22, 343–360, https://doi.org/10.1017/s0954102010000179, 2010.

Rosenblum, E. and Eisenman, I.: Sea Ice Trends in Climate Models Only Accurate in Runs with Biased Global Warming, J. Clim., 30, 6265–6278, https://doi.org/10.1175/jcli-d-16-0455.1, 2017.

Rozema, P. D., Venables, H. J., van de Poll, W. H., Clarke, A., Meredith, M. P., and Buma, A. G. J.: Interannual variability in phytoplankton biomass and species composition in northern Marguerite Bay (West Antarctic Peninsula) is governed by both winter sea ice cover and summer stratification, Limnol. Oceanogr., 62, 235–252, https://doi.org/10.1002/lno.10391, 2017.

Sabbatini, A., Morigi, C., Ravaioli, M., and Negri, A.: Abyssal benthic foraminifera in the Polar Front region (Pacific sector): Faunal composition, standing stock and size structure, Chem. Ecol., 20, 258–271, https://doi.org/10.1080/02757540410001655387, 2004.

Schiebel, R. and Hemleben, C.: Planktic Foraminifers in the Modern Ocean, Springer-Verlag GmbH Berlin Heidelberg, Springer-Verlag GmbH, https://doi.org/10.1007/978-3-662-50297-6, 2017.

Schlosser, E., Haumann, F. A., and Raphael, M. N.: Atmospheric influences on the anomalous 2016 Antarctic sea ice decay, The Cryosphere, 12, 1103–1119, https://doi.org/10.5194/tc-12-1103-2018, 2018.

Seidenkrantz, M.-S.: Benthic foraminifera as palaeo sea-ice indicators in the subarctic realm – examples from the Labrador Sea–Baffin Bay region, Quaternary Sci. Rev., 79, 135–144, https://doi.org/10.1016/j.quascirev.2013.03.014, 2013.

Seidenstein, J. L., Cronin, T. M., Gemery, L., Keigwin, L. D., Pearce, C., Jakobsson, M., Coxall, H. K., Wei, E. A., and Driscoll, N. W.: Late Holocene paleoceanography in the Chukchi and Beaufort Seas, Arctic Ocean, based on benthic foraminifera and ostracodes, Arktos, 4, 1–17, https://doi.org/10.1007/s41063-018-0058-7, 2018.

Smith, R. W., Bianchi, T. S., Allison, M., Savage, C., and Galy, V.: High rates of organic carbon burial in fjord sediments globally, Nat. Geosci., 8, 450–453, https://doi.org/10.1038/ngeo2421, 2015.

Smith, W., Sedwick, P., Arrigo, K., Ainley, D., and Orsi, A.: The Ross Sea in a Sea of Change, Oceanography, 25, 90–103, https://doi.org/10.5670/oceanog.2012.80, 2012.

Smith Jr., W. O., Ainley, D. G., Arrigo, K. R., and Dinniman, M. S.: The oceanography and ecology of the Ross Sea, Ann. Rev. Mar. Sci., 6, 469–487, https://doi.org/10.1146/annurev-marine-010213-135114, 2014.

Stenni, B., Curran, M. A. J., Abram, N. J., Orsi, A., Goursaud, S., Masson-Delmotte, V., Neukom, R., Goosse, H., Divine, D., van Ommen, T., Steig, E. J., Dixon, D. A., Thomas, E. R., Bertler, N. A. N., Isaksson, E., Ekaykin, A., Werner, M., and Frezzotti, M.: Antarctic climate variability on regional and continental scales over the last 2000 years, Clim. Past, 13, 1609–1634, https://doi.org/10.5194/cp-13-1609-2017, 2017.

Tesi, T., Belt, S. T., Gariboldi, K., Muschitiello, F., Smik, L., Finocchiaro, F., Giglio, F., Colizza, E., Gazzurra, G., Giordano, P., Morigi, C., Capotondi, L., Nogarotto, A., Köseoğlu, D., Di Roberto, A., Gallerani, A., and Langone, L.: Resolving sea ice dynamics in the north-western Ross Sea during the last 2.6 ka: From seasonal to millennial timescales, Quaternary Sci. Rev., 237, 106299, https://doi.org/10.1016/j.quascirev.2020.106299, 2020.

Turner, J., Hosking, J. S., Phillips, T., and Marshall, G. J.: Temporal and spatial evolution of the Antarctic sea ice prior to the September 2012 record maximum extent, Geophys. Res. Lett., 40, 5894–5898, https://doi.org/10.1002/2013gl058371, 2013.

Turner, J., Hosking, J. S., Bracegirdle, T. J., Marshall, G. J., and Phillips, T.: Recent changes in Antarctic Sea Ice, Philos. Trans. A Math. Phys. Eng. Sci., 373, 20140163, https://doi.org/10.1098/rsta.2014.0163, 2015.

Turner, J., Phillips, T., Marshall, G. J., Hosking, J. S., Pope, J. O., Bracegirdle, T. J., and Deb, P.: Unprecedented springtime retreat of Antarctic sea ice in 2016, Geophys. Res. Lett., 44, 6868–6875, https://doi.org/10.1002/2017gl073656, 2017.

van Leeuwe, M. A., Tedesco, L., Arrigo, K. R., Assmy, P., Campbell, K., Meiners, K. M., Rintala, J. M., Selz, V., Thomas, D. N., and Stefels, J.: Microalgal community structure and primary production in Arctic and Antarctic sea ice: A synthesis, Elementa Science of the Anthropocene, 6, 4, https://doi.org/10.1525/elementa.267, 2018.

Violanti, D.: Morphogroup Analysis of Recent Agglutinated Foraminifers off Terra Nova Bay, Antarctica (Expedition 1987–1988), in: Ross Sea Ecology, edited by: Faranda, F. M., Guglielmo, L., and Ianora, A., Springer, Berlin, Heidelberg, 479–492, https://doi.org/10.1007/978-3-642-59607-0_34, 2000.

Ward, B. L., Barret, P. J., and Vella, P.: Distribution and ecology of benthic foraminifera in McMurdo Sound, Antarctica, Palaeogeogr. Palaeocl., 58, 139–153, https://doi.org/10.1016/0031-0182(87)90057-5, 1987.

Whitworth, T. and Orsi, A. H.: Antarctic Bottom Water production and export by tides in the Ross Sea, Geophys. Res. Lett., 33, L12609, https://doi.org/10.1029/2006gl026357, 2006.